



Novel structural CYP51 mutation in *Trypanosoma cruzi* associated with multidrug resistance to CYP51 inhibitors and reduced infectivity

Caio H. Franco^{a,b,1}, David C. Warhurst^c, Tapan Bhattacharyya^c, Ho Y.A. Au^c, Hai Le^c, Miriam A. Giardini^d, Bruno S. Pascoalino^a, Ana Claudia Torrecilhas^e, Lavinia M.D. Romera^e, Rafael Pedro Madeira^e, Sergio Schenkman^f, Lucio H. Freitas-Junior^{b,d}, Eric Chatelain^g, Michael A. Miles^c, Carolina B. Moraes^{a,b,d,e,*}

^a Laboratório Nacional de Biociências (LNBio), Centro Nacional de Pesquisa em Energia e Materiais (CNPEM), Campinas, SP, Brazil

^b Department of Microbiology, Institute of Biomedical Sciences, University of São Paulo, São Paulo, SP, Brazil

^c Department of Infection Biology, Faculty of Infectious and Tropical Diseases, London School of Hygiene and Tropical Medicine, London, UK

^d Institut Pasteur Korea, Bundang-gu, Seongnam-si, Gyeonggi-do, Republic of Korea

^e Department of Pharmaceutical Sciences, Federal University of São Paulo (UNIFESP), Diadema, SP, Brazil

^f Department of Microbiology, Immunology and Parasitology, UNIFESP, São Paulo, SP, Brazil

^g Drugs for Neglected Diseases Initiative, Geneva, Switzerland

ARTICLE INFO

Keywords:

Trypanosoma cruzi
Drug resistance
Ravuconazole
Benznidazole
CYP51

ABSTRACT

Ergosterol biosynthesis inhibitors, such as posaconazole and ravuconazole, have been proposed as drug candidates for Chagas disease, a neglected infectious tropical disease caused by the protozoan parasite *Trypanosoma cruzi*. To understand better the mechanism of action and resistance to these inhibitors, a clone of the *T. cruzi* Y strain was cultured under intermittent and increasing concentrations of ravuconazole until phenotypic stability was achieved. The ravuconazole-selected clone exhibited loss in fitness *in vitro* when compared to the wild-type parental clone, as observed in reduced invasion capacity and slowed population growth in both mammalian and insect stages of the parasite. In drug activity assays, the resistant clone was above 300-fold more tolerant to ravuconazole than the sensitive parental clone, when the half-maximum effective concentration (EC₅₀) was considered. The resistant clones also showed reduced virulence *in vivo*, when compared to parental sensitive clones. Cross-resistance to posaconazole and other CYP51 inhibitors, but not to other antichagasic drugs that act independently of CYP51, such as benznidazole and nifurtimox, was also observed. A novel amino acid residue change, T297M, was found in the *TcCYP51* gene in the resistant but not in the sensitive clones. The structural effects of the T297M, and of the previously described P355S residue changes, were modelled to understand their impact on interaction with CYP51 inhibitors.

1. Introduction

Chagas Disease (CD) also known as American trypanosomiasis, is a neglected tropical disease caused by the protozoan parasite *Trypanosoma cruzi*. It is estimated that there are more than six million people infected with *T. cruzi* worldwide, including patients in the endemic regions of Latin America and infected individuals who migrated to non-endemic, developed regions such as parts of North America, Europe, Japan and Australia (WHO, 2013; Antinori et al., 2017; Pérez-Molina and Molina, 2018). As a chronic infection, CD is the parasitic

disease that causes the highest socioeconomic impact in Latin America, with 7–19 billion USD estimated losses in productivity (Lee et al., 2013). The complex *T. cruzi* life cycle involves multiple stages in both vertebrate and invertebrate hosts, with four morphologically distinct forms: in the insect vector, the epimastigotes and metacyclic trypomastigotes, and in the mammalian host, the intracellular amastigotes and blood trypomastigotes. In each host, the cycle progresses with the parasite alternating between replicative, non-invasive forms (epimastigotes and intracellular amastigotes) and nonreplicative, invasive forms (metacyclic and blood trypomastigotes).

* Corresponding author. Carolina Borsoi Moraes: Department of Pharmaceutical Sciences, Federal University of São Paulo (UNIFESP), Diadema, SP, 09913-030, Brazil.

E-mail address: cbmoraes@unifesp.br (C.B. Moraes).

¹ Current address: Centre for Neuroscience and Cell Biology, University of Coimbra, Cantanhede, Portugal.

<https://doi.org/10.1016/j.ijpddr.2020.06.001>

Received 15 January 2019; Received in revised form 29 May 2020; Accepted 4 June 2020

Available online 13 June 2020

2211-3207/© 2020 The Authors. Published by Elsevier Ltd on behalf of Australian Society for Parasitology. This is an open access article under the CC BY-NC-ND license (<http://creativecommons.org/licenses/by-nc-nd/4.0/>).

Table 1
Nomenclature of the culture variants originating from the Y strain clone H10.

Nomenclature	Significance	Drug pressure
H10-S	Parental clone from Y strain (S = ravuconazole sensitive), kept for short term <i>in vitro</i> (max. 8 culture passages after cloning)	N/A
H10-LT	H10-S clone after continuous <i>in vitro</i> culture (LT = long-term), in parallel with H10-R; control for genetic/phenotypic variation/aberration not due to drug pressure)	N/A
H10-R	H10-S clone maintained under increasing and on/off drug pressure, until reaching stable infection levels at 500 nM (R = ravuconazole resistant)	Yes (500 nM ravuconazole, constant pressure after phenotypic stabilization)
H10-R-NP	H10-R for which drug pressure was removed (NP = no pressure); investigation of resistance stability in the absence of drug pressure	No (vehicle only)

CD treatment currently relies on only two drugs: benznidazole and nifurtimox. Both are nitroheterocyclic compounds that were empirically introduced into CD chemotherapy more than four decades ago and, despite often leading to cure when administered during the acute phase of the disease, they are often associated with severe toxicity and limited or unclear efficacy during the chronic phase (Viotti et al., 2006; Pérez-Molina et al., 2009; Yun et al., 2009; Morillo et al., 2015). Furthermore, benznidazole treatment of chronic phase patients with incipient chagasic cardiomyopathy did not appear to improve clinical prognosis (Velazquez et al., 2015).

Considering the disadvantages of current antichagasic chemotherapy, alternative drugs with a safer profile and higher tolerability are critically needed. In recent years, the antifungals posaconazole and E1224, a prodrug of ravuconazole, were the only new drugs to enter clinical trials for CD (Moraes and Franco, 2016). As in fungi, *T. cruzi* uses ergosterol-like lipids as the main sterol in membranes, and ergosterol biosynthesis inhibitors demonstrated anti-*T. cruzi* activity *in vitro* and *in vivo* tests, thus being proposed as candidates for CD chemotherapy (Urbina et al., 2003; Urbina, 2010). However, both drugs presented therapeutic failure in clinical trials for etiological treatment of CD as monotherapy when compared to the standard benznidazole (Molina et al., 2014; Morillo et al., 2017). In parallel to the clinical trials, new data obtained with novel technologies (e.g. more sensitive High Content Screening assays and *in vivo* bioluminescence imaging) have demonstrated that ergosterol biosynthesis inhibitors had indeed limited efficacy against *T. cruzi* both *in vitro* and *in vivo* (Moraes et al., 2014; Francisco et al., 2015; Khare et al., 2015).

Posaconazole and ravuconazole inhibit the sterol 14 α -demethylase cytochrome P450, a functionally conserved CYP monooxygenase member of cytochrome P450 superfamily, also known as CYP51. The CYP enzymes are grouped into one family, and are found in all biological kingdoms, despite overall amino-acid identities from only 22% (Lepesheva and Waterman, 2007). The CYP51 gene is polymorphic in *T. cruzi*, with some parasite strains presenting a single *TcCYP51* copy, such as in the Sylvio strain clones and the subspecies *Trypanosoma cruzi marinkellei*, while others have two copies, A and B, with sequence variation between the copies, such as in Y, CL-Brener and Colombiana strains. In addition, sequence variations can reach up to 16 amino acid differences between distinct strains (Cherkesova et al., 2014).

Drug resistance in infectious diseases is a major clinical issue that affects all classes of microorganisms, including protozoan parasites (Borst and Ouellette, 1995; Purkait et al., 2012). To understand better how sequence variation of *TcCYP51* impacts on *T. cruzi* biology and drug sensitivity, a clone of the Y strain resistant to ravuconazole was selected *in vitro* and analysed genetically and phenotypically.

2. Materials and methods

2.1. Cells and culture

The LLCMK₂ cell line (ATCC, CCL7), the U2OS cell line (obtained from the Rio de Janeiro Cell Bank - BCRJ 0304) and a particular stock of strain Y used in the S. Schenkman, laboratory, which was highly

virulent in mice, were cultured in the mammalian stages as described (Moraes et al., 2014), except that infected tissue cultures were maintained with high glucose DMEM media supplemented with 10% Cosmic Calf Serum (both from Hyclone). Epimastigote forms (Y-strain) were cultured in liver infusion tryptose (LIT) medium, prepared as described (Camargo, 1964), with minor modifications that included 4 g NaCl, 5 g liver infusion broth (Sigma-Aldrich) and 0.8 g glucose (pH 7.2) per liter. The LIT medium was sterilized by autoclaving at 121 °C for 15–20 min and then supplemented with 10% Fetal Bovine Serum (FBS), 100 μ g/mL penicillin and 100 U/mL streptomycin (all from Gibco).

2.2. *Trypanosoma cruzi* cloning

The Y strain was cloned by limiting dilution of tissue culture-derived trypomastigotes. Briefly, LLCMK₂ cells were seeded at non-confluent density in a 96-well microplates (Greiner BiOne). After 24 h, Y strain trypomastigotes were serially diluted at a factor of 10-fold, to isolate individual parasites by limiting dilution, and plated onto LLCMK₂ for infection. After approximately two weeks, trypomastigotes could be observed in the supernatant in some of the infected wells, at expected rates. Several clones were selected and propagated in LLCMK₂ tissue cultures, as described above.

2.3. Selection of ravuconazole resistance

Table 1 indicates the clones used in this study and their nomenclatures. One of the Y clones generated, H10 (identified as H10-S in this study), was chosen for selection of resistance to ravuconazole due to its rapid growth *in vitro* when compared to the parental Y strain (data not shown). Resistance to ravuconazole was selected at the mammalian stages for a period of approximately 12 months. During this period, two H10-infected LLCMK₂ cultures were maintained in parallel, one under intermittent drug pressure, at increasing concentrations, starting at 1 nM; the other culture (H10-LT) was maintained with vehicle (DMSO) pressure, with concentrations adjusted to match the DMSO concentration in the drug-treated flask. Fresh tissue cultures were prepared as needed and infected with trypomastigotes. Throughout the selection of resistance, culture media (with or without drug) was changed every 3–4 days. Eventually, the drug-treated cultures would not produce trypomastigotes for extended periods (more than 2 weeks), at which point drug pressure was removed until trypomastigotes were observed in the supernatant. Drug pressure was increased progressively until 1 μ M ravuconazole, and several stocks of intermediate resistance were isolated during the process. The stocks isolated at drug pressure of 500 nM and 1 μ M ravuconazole were further maintained at constant drug pressure for another 3 months to increase phenotypic stability, which was evaluated quantitatively (i.e., regarding the number of trypomastigotes released from infected cultures, and the intracellular cycle length). However, the stock growing under 1 μ M ravuconazole did not reach phenotypic stability in levels compatible with the subsequent infection assays (see below), and thus the stock growing at 500 nM ravuconazole was selected as the resistant clone (H10-R). At this point, a stock of

H10-R was isolated in a separate culture flask and maintained off-drug pressure. This stock (H10-R-NP) was then cultured continuously *in vitro*, in the presence of 0.01% DMSO, in parallel to H10-R culture.

2.4. Trypomastigote to epimastigote differentiation and epimastigote growth curves

Tissue culture-derived trypomastigotes were collected from infected LLCMK₂ culture flasks, centrifuged, resuspended in LIT medium in culture flasks at the density of 5×10^5 trypomastigotes/mL and incubated at 28 °C. Manual counts of epimastigotes were performed daily for 17 days. The growth curve count started with the initial density of 1.0×10^5 epimastigotes/mL for all clones while cultured in T25 culture flasks. These counts were performed in duplicate (two independent counts) and in doublets (two different culture flasks counted per day). Epimastigote doubling time was based on the ratio between the growth period of 48 h (during exponential growth) and the number of generations (n), which can be calculated according to the following two equations: (1) Doubling Time (dt) = culture growth period/n; and (2) $n = \frac{\ln X_{\text{final}} - \ln Y_{\text{initial}}}{0.693}$, where X-final and Y-initial refer to the parasite counts on the last and first days of exponential growth in culture, respectively. The same equation was applied for calculation of amastigote doubling times, except that a 72h period was used instead.

2.5. Metacyclogenesis

The epimastigote cultures of H10-S, H10-LT, H10-R and H10-R-NP were centrifuged and re-suspended in Grace's medium (Vitrocell), supplemented with 10% FBS, 100 µg/mL penicillin and 100 U/mL streptomycin (all from Gibco). Cultures were maintained at 28 °C. Visual inspections were performed on a daily basis and eventually metacyclic trypomastigotes were evident in the culture. Metacyclic trypomastigotes were transferred to fresh nonconfluent LLCMK₂ culture flasks at least 5:1 (metacyclic trypos: host cell) ratio.

2.6. Compounds

Benznidazole was provided by Nortec Química; nifurtimox, posaconazole, EPL-BS967, EPL-BS497/AN4169 and EPL-BS1246 were obtained from Epichem Pty; ravuconazole was donated by Eisai Ltd. Amphotericin B, fluconazole, itraconazole, ketoconazole and voriconazole were obtained from Sigma-Aldrich. All compounds were in solid state and dissolved in the appropriate volume of dimethyl sulfoxide (DMSO, Sigma-Aldrich) to prepare stock solutions at 10 mM, except for benznidazole (40 mM), posaconazole and ravuconazole (both at 8 mM). All aliquots were stored at – 80 °C, protected from light, and subjected to no more than three cycles of freezing-thawing to ensure the chemical integrity of the compounds.

2.7. Antiparasitic assay

The anti-*T. cruzi* assay was performed as described (Silva et al., 2016), with minimal changes. Trypomastigotes were added at 28,000 trypomastigotes/well for H10-R and H10-NP, and at 14,000 trypomastigotes/well for H10-S and H10-LT clones. When these assays were performed, clone H10-R-NP had been grown in drug-free culture medium for 48 days. Compounds were 2-fold diluted and tested in 20 concentrations to generate dose-response curves, starting either at 400 µM (benznidazole), 8 µM (posaconazole and ravuconazole) and 100 µM (all other compounds). Following compound addition, assay plates were incubated for 96 h under 37 °C and 5% CO₂. Negative control wells (infected cells) and positive control wells (noninfected cells) were treated with 1% DMSO only. Every assay was performed at least in duplicate (two independent experiments).

2.8. Image acquisition & processing and data analysis

Plates were imaged with the Operetta high content system (PerkinElmer), with 5 images/well were acquired under the 20x magnification lens (long working distance). Xenon laser was set to 90% of excitation (lamp power), 0% transmission; the filter wavelengths were 620–640 nm for excitation and 650–760 nm for emission (far red) and the set exposure time for imaging was 800 ms. The images were processed using Harmony® (PerkinElmer) to identify, segment and quantify the nucleus and cytoplasm of host cells, as well as to perform the detection and counting of amastigotes present within the cytoplasmic region. The output data provided by HCA cover all images acquired per well and quantifies the total number of cells, total number of infected cells, total number of intracellular parasites, as well as the mean number of parasites/cell and their standard deviation. To calculate the infectivity efficiency of each clone, an infectivity index was used, by dividing the ratio of infected cells for the control wells and the trypomastigote-to-U2OS ratio used at the infection for each of the clones. Output data were organized and processed using Excel (Microsoft Office). All plots were prepared with the Prism Graphpad, version 6. EC₅₀ is a measurement of potency and was defined as the compound concentration corresponding to 50% of normalized activity (or 50% reduction in infection ratio), after 96 h of compound incubation. Maximum activity (MA) is a measurement of efficacy and was defined as the highest value of antiparasitic activity observed for a given compound.

2.9. Extraction of genomic DNA

Extraction of genomic DNA from epimastigote cultures of H10-S, H10-LT, H10-R, H10-R-NP, and stocks resistant to other ravuconazole concentrations (4 nM, 8 nM and 1 µM) was performed using the Gentra kit Puregene Blood Kit (Qiagen) following the manufacturer's recommendations, according to the guidelines outlined from Pacific BIOSCIENCES™ (PacBio) (Yuan, 2012) and indicated for preparation of samples for single-molecule real time (SMRT) sequencing.

2.10. Genotyping

The genetic lineage (discrete typing unit, DTU) TcII of the susceptible *T. cruzi* Y strain was determined by PCR-RFLP of the heat shock protein 60 (*HSP60*) and glucose phosphate isomerase (*GPI*) genes (Lewis et al., 2009) and by sequencing of the trypomastigote small surface antigen gene (*TSSA*), generated using primers T5/ATG/E an EMT/5 (Di Noia et al., 2002). The genotype of all the derived resistant clones was verified as TcII by the same methods (Supplementary Fig. S1).

2.11. PCR amplification and DNA sequencing of the CYP51 gene

Primers used for the amplification of the TcII Y strain were based on those described for the Tulahuen strain (TcII) CYP51 sequence (GenBank Accession AY856083) (Lepesheva et al., 2006), as listed in Table S2. Primers TcCYP51Forward and TcCYP51Reverse were used to amplify the entire 1446 nucleotide coding sequence, including stop codon, and to sequence the subsequent amplicon, in conjunction with the internal primers TcCYP51int-1 to – 4. Amplification reactions were performed in a total volume of 20 µl and comprised of 1 x NH₄ reaction buffer supplemented with 1.5 mM MgCl₂ (Bioline), 200 µM dNTPs (New England Biolabs), 10 pmol of primers TcCYP51For and TcCYP51Rev, and 1 U BioTaq DNA polymerase (Bioline). Amplification conditions were: 1 cycle of 94 °C, 3 min; 25 cycles of 94 °C for 30 s; 55 °C for 30 s; 72 °C for 30 s. Five microliters of the PCR reaction were analysed by electrophoresis on 1.5% agarose gels (Bioline); amplification products were purified from the remaining reaction by precipitation with an equal volume of isopropanol at room temperature,

followed by washing with 70% EtOH, air-drying and resuspension in ddH₂O. Bi-directional DNA sequencing, using each PCR and internal primer separately at 3.2 pmol, was achieved using a BigDye Terminator v3.1 RR-100 kit (Applied Biosystems) according to standard protocols. Sequence alignment was performed using BioEdit software (Hall, 1999). GenBank sequences JQ434483 (Y strain CYP51A) and JQ434484 (CYP51B), from (Cherkesova et al., 2014), were aligned to identify polymorphisms that could be exploited for incorporation at the 3' end of CYP51A-specific PCR primers. The PCR templates used included those of the drug resistant mutants. Additionally, as described by (Cherkesova et al., 2014), primers binding to sequences at the 5' and 3' ends common to both A and B forms were used to generate an amplicon that was then plasmid cloned (pGEM T-easy, Promega), and multiple clones derived from plasmids were sequenced.

2.12. Analysis of protein structure

Residue side chain intrinsic hydrophilicity/hydrophobicity values at pH 7.0 in 10 mM phosphate buffer were derived from Table III published by Kovacs and collaborators (Kovacs et al., 2006). Measurement of residue side-chain volumes was carried out in the HyperChem 8 QSAR programme (Hypercube Inc.). The amino acid structures were obtained from the HyperChem database, and volume in Å³ was measured after the backbone amino- and carboxylic acid groups had been removed from the α-Carbon, and replaced by protons. BLAST and CLUSTAL-0 ALIGNMENT were carried out on the ExPasy site. Representation of *.pdb structures of crystals deposited in the RCSB data bank (<http://www.rcsb.org/pdb/explore.do>) was carried out using DeepView the Swiss Model programme (<http://spdbv.vital-it.ch/>). In all cases where more than one strand was represented the A strand was used. The impact of residue changes on crystal structures was determined using the program “DUET” (Pires et al., 2014), which measures Gibbs energy change (delta delta Gibbs, δδG) (in kcal/mol) involved in folding and unfolding a wild-type or mutated structure, considering the overall energy in the wild-type as zero, and comparing the increase or decrease of energy in the mutant. This provides a positive (stabilising) or negative (destabilising) value for the new residue. Very positive or negative ddG values are likely to render a protein less fit: most common non-damaging mutations are between + or – 1.0. In utilising the DUET server (Pires et al., 2014) for residue-change in the demethylase enzyme crystal structure, initially for T297M change, on triazole (posaconazole) 3k1o.pdb, pyridine (UDO) 3zg2.pdb and triazole (fluconazole) 3kkm.pdb, we regarded it as essential to delete the heme and drug ligands from the crystal structures used before accessing the server. Running the DUET procedure in the presence of the ligands, although there was actually no difference in ddG result, produced undesirable changes in both heme and drug structures, possibly casting doubt on the results. Selected aspects of the following CYP51 crystal structures were analysed: (i) the crystal structure of human lanosterol 14-alpha demethylase [3juv.pdb]; the same protein ligated with the imidazole econazole BCD [3jus.pdb], and the human protein ligated with the imidazole ketoconazole [3Ld6.pdb]; (ii) *T. cruzi* CYP51 crystal structure ligated with triazole posaconazole [3k1o.pdb]; (iii) an alternative *T. cruzi* crystal structure ligated with fluconazole [3kkm.pdb], and ligated with the diazole VNF [3ksw.pdb]; (iv) the alternative structure ligated with pyridine UDO [3zg2.pdb] or pyridine UDD [3zg3.pdb A]; and (v) the *T. brucei* structure ligated with imidazoles VNI [3gw9.pdb] and VFV [4g7g.pdb].

2.13. In vivo infection

BALB/c female mice (8–10 week-old) were obtained from the animal facility at the CEDEME- Federal University of São Paulo (UNIFESP). All the animal handling and procedures were approved by the Committee on the Ethical handling of laboratory animals – CEUA-UNIFESP, Diadema, São Paulo, Brazil (protocol 1535130318). *T. cruzi*, Y strain

was routinely maintained by weekly intraperitoneal (i.p.) infection of BALB/c mice. The Y strain clones were passed for one cycle in BALB/C mice, and blood trypomastigotes were collected during parasitemia peak. Parasitemia was quantified by counting motile parasites in 5 µl of fresh blood sample drawn from lateral tail veins. For the profiling of *in vivo* infection, inoculation was performed by injecting 10,000 blood forms from Y strain and from each clone H10–S, H10-LT, H10-R, H10-R-NP. In control groups, mice were inoculated only with Y strain blood forms. Peripheral blood was collected from infected animals and parasitaemia was determined by optical microscopy until day 15 post infection. Motile parasites were counted from 5 fields of the slide and the total counting value was multiplied by a correction factor established according to microscope objective, diameter and coverslip area to obtain the number of parasites/mL. Survival was assessed daily from day 0–30 post-infection; all remaining animals were euthanized. Data were analysed using software GraphPad Prism version 7.

3. Results

3.1. Drug susceptibility of *T. cruzi* clones

A *T. cruzi* Y strain clone, H10, was selected by limiting dilution and cultured *in vitro* under on-off increasing ravuconazole pressure. At several points during the selection process, stocks of the resistant population were prepared for genetic and phenotypic characterization. In parallel to the selection of resistant clones, a stock of the parental clone was kept under continuous culture to control for possible alterations due to prolonged *in vitro* culturing. The selection process was progressed up to the point when cultures were growing in the presence of 1 µM ravuconazole. However, the stocks growing under 1 µM ravuconazole produced a remarkably low number of trypomastigotes from infected tissue cultures, when compared to the sensitive parental stock. The low trypomastigote production was not compatible with the phenotypic characterization of drug resistance (data not shown), and thus the stock maintained under 500 nM ravuconazole was selected for phenotypic and genetic characterization of resistance. As this resistant stock was growing stably *in vitro*, it was derived into two subpopulations: one under constant 500 nM ravuconazole pressure, and another kept off-ravuconazole for a period of approximately 10 weeks.

The sensitive and resistant populations of H10 clones were characterized phenotypically in high content assays, which enable automated and robust analysis of intracellular infection. The two stocks of parental clones, H10–S (with limited *in vitro* passaging) and H10-LT (with continuous *in vitro* passaging) presented a susceptibility to ravuconazole consistent with a sensitive phenotype (Table 2), with no significant differences between them. In contrast, the ravuconazole-resistant clone (H10-R) showed greatly increased tolerance to ravuconazole, in comparison with the sensitive clones. At four days of exposure to ravuconazole in dose-response, the EC₅₀ for H10-R clone could not be determined as the drug did not reach 50% of activity within the tested concentration (and plateaued at about 35% activity),

Table 2
T. cruzi H10 clones and their susceptibility to ravuconazole.

Y strain clone		Exposure to ravuconazole – intracellular amastigotes – 96 h	
Designation	Remarks	EC ₅₀ (nM)	^a MA (%)
H10–S	Parental clone	5.4	86.9
H10-LT	Parental clone in long term culture	7.7	78.6
H10-R	Cultured in 500 nM ravuconazole	^b ND	36.4
H10-R-NP	H10-R off ravuconazole (“no pressure”)	2,920	71.5

^aMA, maximum activity; ^bND: values could not be calculated/determined.

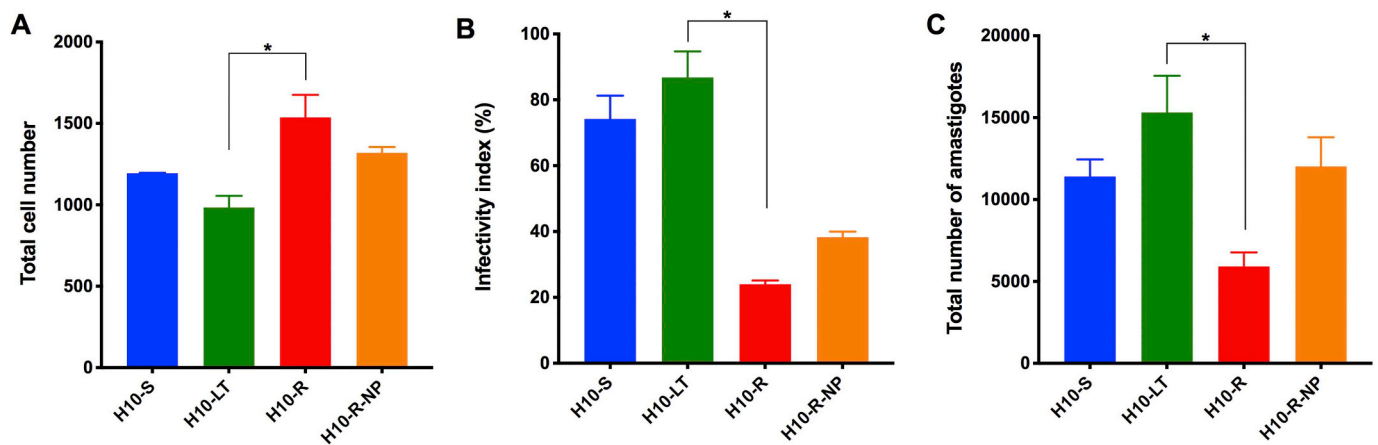


Fig. 1. Phenotypic evaluation of *T. cruzi* ravuconazole-sensitive and resistant clone infections in the absence of drug pressure. Infection of the human host cell line, U2OS, was evaluated by high content analysis at 120 h post-infection for the sensitive (H10-S, blue, and H10-LT, green) and resistant (H10-R, red, and H10-R-NP, orange) Y strain H10 clones. (A) Total number of U2OS host cells. (B) The infectivity index shows the infection ratio divided by the number of trypomastigotes used for infection of tissue cultures for each clone (MOI). The index is normalized and presented in percentage. (C) Total number of amastigotes in the population. Values refer to mean (bars) \pm standard deviation (error bars) obtained in two independent experiments; * indicates statistically significant differences through one-way ANOVA ($P < 0.05$). (For interpretation of the references to colour in this figure legend, the reader is referred to the Web version of this article.)

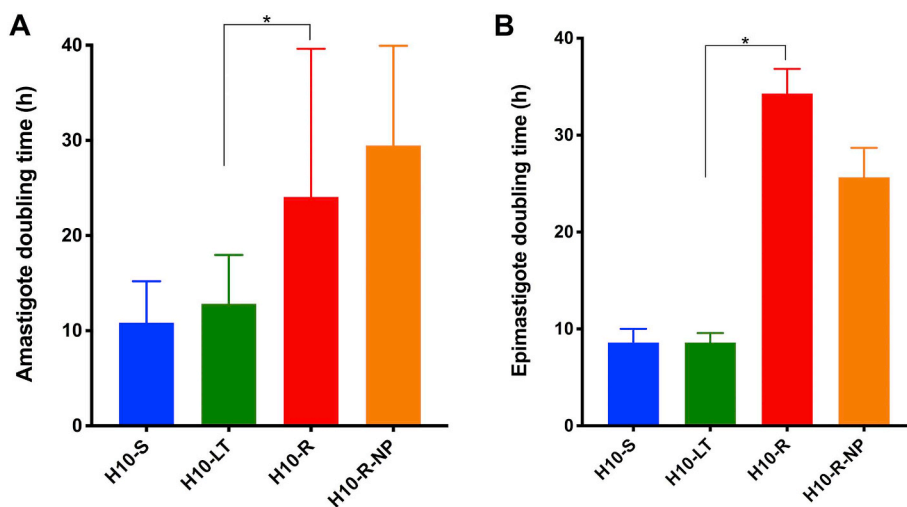


Fig. 2. Resistance to ravuconazole correlates with reduced growth in both amastigotes and epimastigotes. H10-S clone is shown in blue, H10-LT is in green, H10-R is in red and H10-R-NP is in purple. (A) Mean amastigote population doubling time (in hours; Y-axis), calculated based on a 72-h growth curve (without ravuconazole) for each Y strain H10 clone. (B) Mean epimastigote population doubling time (in hours; Y-axis), calculated based on a 48-h interval during epimastigote exponential growth (X-axis). Error bar indicates the standard error from independent counts; * indicates statistically significant differences through one-way ANOVA ($P < 0.05$). (For interpretation of the references to colour in this figure legend, the reader is referred to the Web version of this article.)

while the EC_{50} for sensitive clones was within low nanomolar range (7.7 nM for H10-LT and 5.4 nM for H10-S). The removal of ravuconazole pressure was not sufficient to restore sensitivity to the drug, as the ravuconazole EC_{50} for resistant clone culture off-ravuconazole (H10-R-NP) was determined at approximately 2.9 μ M, still more than 300 times higher than the values observed for the sensitive clones. Likewise, long-term cultivation *in vitro* did not cause the emergence of drug resistance, as the H10-S (parental) and H10-LT clones were similarly susceptible to ravuconazole.

3.2. Ravuconazole resistance in *T. cruzi* is associated with reduced growth and infectivity

The fitness of each H10 clone was also evaluated by means of a multiparametric quantitative analysis of their *in vitro* infection in U2OS cells (Fig. 1). The infection by the resistant clone, H10-R, was associated with an increased number of host cells, indicating a reduction in the cytopathic activity, compared to that often observed for the *T. cruzi* Y strain (Fig. 1A), and reduced infectivity, as seen by the lower infectivity index (the normalized ratio of infected cells, Fig. 1B) and lower number of intracellular amastigotes, when compared to the sensitive clones (Fig. 1C), H10-S and H10-LT. The off-drug resistant clone (H10-R-NP) infection was associated with higher number of amastigotes

when compared to H10-R, but also with a reduced infectivity when compared to the sensitive clones. These data suggest that the removal of ravuconazole pressure from culture could partially restore the fitness of the resistant *T. cruzi* clone, likely by means of increased growth capacity (i.e., amastigote multiplication), but not the invasion capacity as originally observed for the parental, sensitive H10-S clone. In other words, although the H10-R clone is tolerant to the drug, the presence of ravuconazole in culture media still affects the intracellular parasite growth. This could also be observed in the trypomastigote yield from infected tissue cultures, as it was clear that H10-S and H10-LT were producing 10 to 20 times more trypomastigotes per volume of culture, when compared to H10-R and H10-R-NP (data not shown). As observed for drug sensitivity, the long-term cultivation of Y strain clones did not cause the phenotype of reduced growth and infectivity; on the contrary, the prolonged *in vitro* culture favored increased invasion and amastigote growth rates, as seen by the infection profile obtained with the H10-LT clone in comparison with the parental H10-S clone.

The correlation between reduced growth and resistance to ravuconazole was further investigated by estimating the population doubling time for *T. cruzi* replicative forms, amastigotes and epimastigotes (Fig. 2). The mean population doubling time of amastigotes and epimastigotes was of approximately 12 h for both amastigotes and epimastigotes for H10-S and H10-LT sensitive clones (Fig. 2A and B),

again demonstrating that the prolonged *in vitro* culture did not alter *T. cruzi* growth capacity significantly in either life cycle stage. As expected, the ravuconazole-resistant clones, H10-R and H10-R-NP, were associated with longer doubling times when compared to sensitive clones, with mean population doubling times of 18–20 h in the amastigote and, curiously, an even longer mean doubling time of 26–29 h in the epimastigote stage. The epimastigotes from H10-R and H10-R-NP also seemed to reach stationary growth phase in culture at approximately 1×10^7 epimastigotes/mL, while the sensitive H10-S and H10-LT clones would continue to grow exponentially beyond those densities during the period evaluated (data not shown).

Despite the reduced growth observed in H10-R and H10-R-NP, all clones were capable of differentiating from tissue culture trypomastigotes to epimastigotes, and then from epimastigotes to metacyclic trypomastigotes (data not shown), with some differences. In particular, during the attempt to differentiate clones from tissue culture trypomastigotes into epimastigote forms, it was noted that the H10-R differentiation process was markedly slower than that observed for the sensitive clones, H10-S and H10-LT clones (data not shown). Under the same experimental conditions, a period of two to three days was sufficient for the complete differentiation of trypomastigotes into epimastigotes for sensitive H10-S and H10-LT clones, followed by a lag phase of two to four days before starting exponential growth. However, for the resistant clones, six days were required for the complete differentiation of tissue culture trypomastigotes to epimastigotes, followed by a lag phase of at least six days (data not shown). The resistant clones also showed a greater degree of morphological abnormalities during the differentiation process (data not shown). Interestingly, the differentiation of tissue culture trypomastigotes to epimastigotes did not occur in the presence of 500 nM ravuconazole, even in the resistant clone H10-R (data not shown), suggesting that *TcCYP51* and ergosterol play a vital role in membrane remodelling during differentiation, and that the resistance to ravuconazole observed in amastigotes was not sufficient to prevent inhibition of *TcCYP51* by ravuconazole during the differentiation process.

The clones' virulence was then evaluated in a mouse model of acute infection, using the parental Y strain as control. The animals were infected with 10,000 trypomastigotes of either the parental strain Y or the H10-S, H10-LT, H10-R-NP and H10-R clones. The group of animals that were infected with either the parental strain Y or the sensitive clones, H10-S and H10-LT, showed an earlier parasitemia peak (day 9 post-infection) when compared to the group infected with the resistant clones H10-R and H10-R-NP (day 13 post-infection – Fig. 3). While sensitive clones peaked at the same day as the parental Y strain, the latter produced about 10-fold more trypomastigotes than the former; despite the delay in the parasitemia peak, resistant clones produced blood trypomastigotes at similar levels to the sensitive clones. Animals that were infected with the clones had a survival rate of 100% while animals infected with the parental Y strain had a survival rate of 20% on day 30 after infection. This was probably due to a progressive loss of virulence due the continues passage *in vitro*, independently of the resistance to ravuconazole.

3.3. Ravuconazole-resistance confers cross-resistance to other azoles and non-azoles CYP51 inhibitors

The susceptibility of clones to other reference drugs, benznidazole, nifurtimox and posaconazole, was then determined. These clones presented increased resistance (or tolerance) to posaconazole (Table 3). The ravuconazole-resistant clones, H10-R and H10-R-NP showed a remarkable degree of resistance to posaconazole, with EC_{50} values ranging from 1 to 2 nM in the sensitive clones to 1.8–17 μ M in the resistant clone. The maximum activity observed for posaconazole was moderate and similar for all clones, with levels ranging from approximately 65%–85%. However, to achieve these levels of activity, resistant clones required exposure to posaconazole concentrations that were

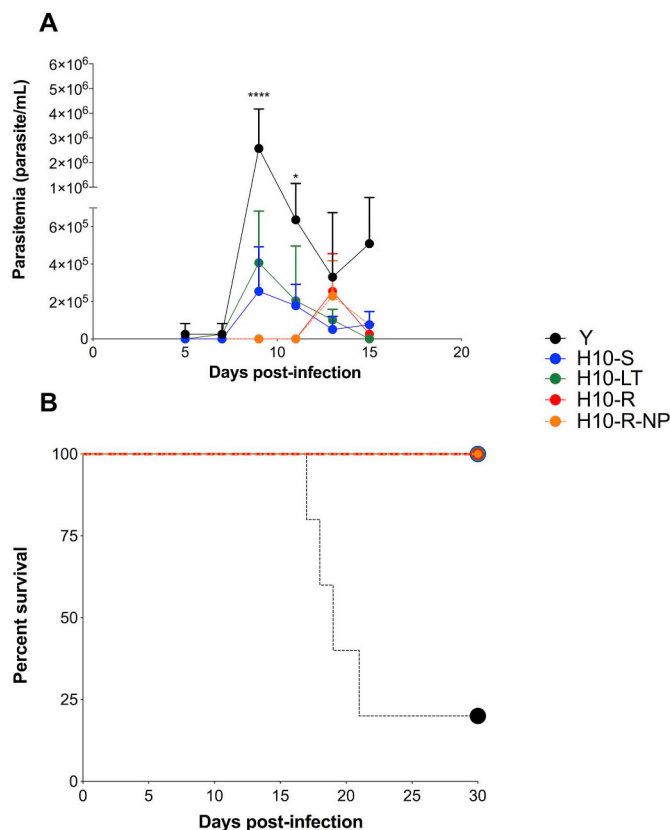


Fig. 3. Ravuconazole-resistant clones delayed parasitemia peak *in vivo* when compared to the sensitive clones. Parasitemia (A) and percent survival (B) of animals infected with strain Y and H10-S, H10-LT, H10-R-NP and H10-R clones. Animals were infected with 10,000 forms from each Y strain and H10-S, H10-LT, H10-R, H10-R-NP clones. Peripheral blood was collected from infected animals and parasitaemia determined by optical microscopy until day 15 post infection. Survival followed each group until day 30 post infection.

Table 3

EC_{50} values and maximum activity (MA) of benznidazole, nifurtimox and posaconazole against H10 clones.

Clone	Benznidazole		Nifurtimox		Posaconazole	
	EC_{50} (μ M)	MA (%)	EC_{50} (μ M)	MA (%)	EC_{50} (nM)	MA (%)
H10-S	31.4	96.2	3.5	95.2	2.1	85.7
H10-LT	41.8	88.2	3.3	94.4	1.2	75.9
H10-R	42.5	83.3	6.1	83.6	17,159	65.5
H10-R-NP	28.0	89.7	2.4	95.2	1,811	80.5

approximately 1000 times higher than those necessary for sensitive clones. In contrast, no significant difference in level of susceptibility to benznidazole was observed between sensitive (H10-S and H10-LT) and resistant (H10-R and H10-R-NP) clones, suggesting that these clones were naturally tolerant to benznidazole, a phenotype that has been previously reported for the Y strain of *T. cruzi* (Filardi and Brener, 1987). A similar pattern of tolerance, albeit in a much lower and perhaps non-significant degree, was observed for nifurtimox, with EC_{50} values varying from approximately 2 to 6 μ M and maximum activities ranging from 83% to 95% (Table 3), which is slightly lower than maximum activity (approx.100% at 96 h) observed for nifurtimox across a panel of *T. cruzi* strains (Morales et al., 2014). As for benznidazole, there were no significant differences in the levels of nifurtimox activity among the different clones.

In conclusion, the level of resistance observed to posaconazole was similar to that observed for ravuconazole when comparing sensitive and

resistant clones, and altogether these data show that resistance to ravuconazole can lead to cross-resistance to posaconazole, but not to the nitroheterocyclic drugs benznidazole and nifurtimox. Conversely, natural resistance or tolerance to benznidazole does not confer cross-resistance to azoles. Furthermore, long-term cultivation of *T. cruzi* *in vitro* did not alter the naturally acquired tolerance/resistance phenotype for benznidazole, as demonstrated by the drug profiling in the sensitive H10-LT clone in comparison to the parental H10-S clone, and removal of ravuconazole pressure did not lead to a significant rescue in susceptibility to azoles.

The spectrum of the drug resistance in the clones was investigated further in comparison with other compounds that are known CYP51 inhibitors – other triazoles (fluconazole, itraconazole and voriconazole), the imidazole ketoconazole and the fenarimols EPL-BS967/UDO and EPL-BS1246/UDO, all previously reported as having anti-*T. cruzi* activity (McCabe et al., 1986; Goad et al., 1989; Buckner et al., 1998; Gulin et al., 2013; Moraes et al., 2014). The polyene antibiotic amphotericin B, an antifungal reported to have moderate anti-*T. cruzi* activity (Buckner et al., 1998; Yardley and Croft, 1999; Cencig et al., 2011; Clemons et al., 2017), AN4169/EPL-BS497, an antichagasic oxaborole lead compound that has broad-spectrum anti-*T. cruzi* activity but does not inhibit CYP51 (Moraes et al., 2014; and data not shown), and the fenarimols, which have been shown to have moderate anti-*T. cruzi* activity by inhibiting CYP51 (Keenan et al., 2012; Hargrove et al., 2013) were also tested. The results showed that the resistant clone H10-R is also cross resistant to other triazole (fluconazole, itraconazole and voriconazole), imidazole (ketoconazole) and the two fenarimol (EPL-BS967 and EPL-BS1246) CYP51 inhibitors (Table 4). The EC₅₀ values increased by at least one order of magnitude for these compounds, but with no substantial differences in the maximum activity was observed for each drug in resistant in comparison to sensitive clones. UDO had an EC₅₀ value approximately 88 times higher for H10-R clone (17.7 μM) in comparison with H10-S clone (0.2 μM). Less variation was observed for UDD, with the EC₅₀ ratio 45 times higher for H10-R clone when contrasted with H10-S; nonetheless, both fenarimols showed reduced efficacy against the resistant clone, when compared to the sensitive clone. The increased tolerance to fenarimol derived compounds indicates that the resistance is not restricted to triazole and imidazole-derived compound classes.

Interestingly, amphotericin B showed only reduced activity against either the sensitive or the resistant H10 clone, with maximum activity values between 35% and 40%. Although amphotericin B has been shown to inhibit the growth of *T. cruzi* (De-Castro et al., 1993; Cencig et al., 2011), it does not seem to inhibit CYP51 and rather depends on the presence of ergosterol to exert activity, as it is likely to bind membrane ergosterol and form pores that result in cell lysis (Buckner et al., 1998; Haido and Barreto-Berger, 1989). No significant variations were observed for compound AN4169 in terms of potency and efficacy among the H10 clones, which indicates that the specific target of this

Table 4

Anti-*T. cruzi* activity of amphotericin B, azoles, fenarimols and oxaborole against the sensitive and the resistant H10 clone.

	H10-S		H10-R	
	EC ₅₀ (μM)	MA (%)	EC ₅₀ (μM)	MA (%)
Fluconazole	9.3	68	ND ^a	30
Itraconazole	0.1	102	6.2	87
Voriconazole	0.2	73	ND ^a	56
Ketoconazole	0.04	65	4.5	63
BS967/UDO	0.5	91	22.8	65
BS1246/UDO	0.2	86	17.7	72
Amphotericin B	ND ^a	36	ND ^a	33
AN4169	1.8	89	0.7	84

^aND indicates that the value could not be calculated. Data from two independent experiments.

compound possibly was not affected in the resistance development process.

Changes in gene expression patterns, chromatin organization and quantity of nuclear DNA has been shown to occur during the life cycle of protozoa, including *T. cruzi* (Daniels et al., 2010). As the resistance could also be attributed to non-genetic or epigenetic mechanisms, the stability of the azole-resistant phenotype was further determined by submitting all clones to a full *in vitro* life cycle. Epimastigotes were differentiated to metacyclic trypomastigotes and used to infect fresh tissue cultures. The released tissue-derived trypomastigotes were then harvested and submitted to drug susceptibility phenotypic assays. The results are shown in Table S1. Overall, the levels of susceptibility of all clones to ravuconazole, benznidazole, nifurtimox and posaconazole were maintained after the completion of a full *in vitro* cycle. No significant quantitative or qualitative phenotypic differences in terms of differentiation to metacyclics among the different clones were observed. Trypomastigote yield from infected tissue cultures was at similar levels before and after cycling (data not shown). Altogether, the body of data demonstrated that the changes that lead to the development of resistance to azoles and phenotypic alteration of infectivity and replication rates were stable and could be sustained, suggesting that the resistance phenotype was mainly of a genetic nature.

3.4. Identification of a novel CYP51 mutation

To confirm the potential genetic nature of the resistance phenotype, *TcCYP51* sequences derived from the ravuconazole sensitive clone (H10-LT), the principal resistant clone (cultured under 500 nM ravuconazole) and other four resistant clones isolated during the resistance selection process, cultured under pressure of intermediary concentrations of ravuconazole, were analysed. The sequences have been submitted to GenBank (accession numbers MH998377 (H10-LT), MH998378 (H10-R 4 nM), MH998379 (H10-R 8 nM), MH998380 (H10-R 1 μM), MH998381 (H10-R 500 nM) and MH998382 (H10-R-NP). Primers pairs designed on the basis of published CYP51A sequences to favour amplification of CYP51A yielded no CYP51A amplicons, only CYP51B. Furthermore, the entire open reading frame of CYP51 from the H10-R 500 nM resistant clone was amplified and cloned into plasmids: CYP51A-specific sequences (GenBank JQ434483) divergent from CYP51B (JQ434484) were not identified in any of 27 plasmid clones.

A previously unreported nucleotide heterozygosity, C890T, was identified in all the resistant clones, but not in the sensitive clone (H10-S or H10-LT). This mutation is predicted to lead to an alteration of the encoded amino acid in the CYP51 protein from Thr to Met at position 297 - T297M (Fig. 4). The P355S residue change in CYP1A of resistant clones reported by Cherkesova and collaborators (Cherkesova et al., 2014), which would be due to nucleotide change C1063T, was not observed here in any of the ravuconazole resistant clones (Fig. 4), nor in any of the 27 plasmid clones derived from the H10-R. However, the novel C890T nucleotide heterozygosity was confirmed with plasmid clones having either C (14 clones) or T (13 clones) at that site.

Comparison of *T. cruzi* CYP51 sequences available in GenBank revealed the presence of a number of point mutations throughout the extent of the protein, but only the P355S reported by Cherkesova and collaborators (Cherkesova et al., 2014) and the T297M identified in this study were reported in *T. cruzi*, specifically in the *Y* strain (*TcII*). Point mutations in positions 297 and 355 of the protein sequence were not observed in studies with *T. cruzi* strains *Colombiana* (*TcI*) (Soeiro et al., 2013), *Dm28c* (*TcI*) (Grisard et al., 2014), *Silvio* (*TcI*) (Franzén et al., 2011), *CL Brener* (*TcVI*) (El-Sayed et al., 2005) and *Tulahuen* (*TcVI*) (Buckner et al., 2003; Lepesheva et al., 2006) (Table 5). Fig. 5 presents alignments of amino acid sequences of CYP51 from two fungal species, *Candida albicans* and *Aspergillus fumigatus*, humans and *T. cruzi*. The annotation of Fig. 5 and its accompanying legend indicate: the structural features (helix; β-strand; Turn:TT); the cytochrome binding sites; the drug binding sites; the conserved signature regions; the adjacent

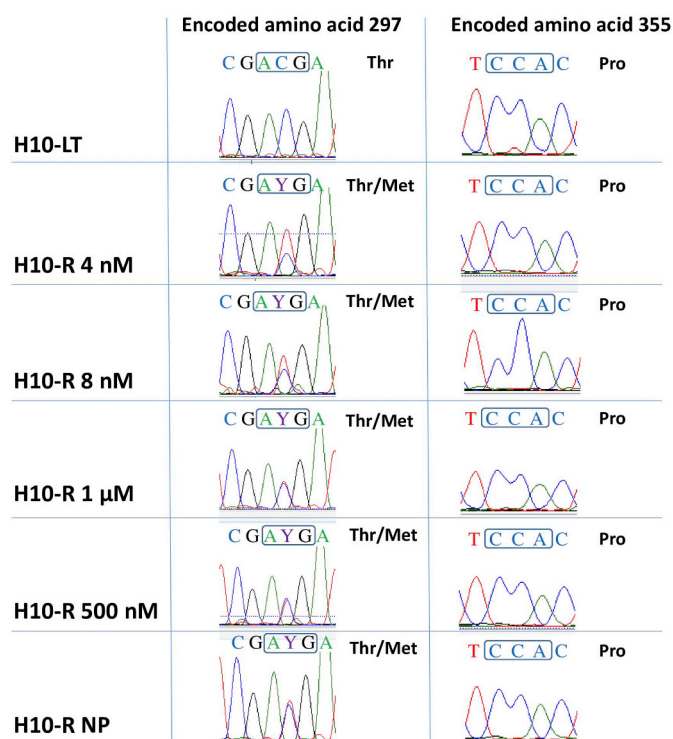


Fig. 4. A novel mutation, T297M, detected by direct sequencing of the CYP51 PCR product of *T. cruzi* Y strain H10-R clones. The T297M mutation is associated with broad-spectrum resistance to CYP51 inhibitors. Left panel: the codon for amino acid 297 (boxed) is mutated from ACG in the wild-type to AYG in the resistant clones, where Y = C + T. Right panel: the previously described mutation in the codon for amino acid 355, which would change CCA to TCA, (boxed) was not present. The *TcCYP51* genes were sequenced of sensitive (H10-LT) and the resistant (H10-R 500 nM ravuconazole and H10-R-NP) clones, along with other clones that were isolated, either earlier (H10- 4 nM and H10-R 8 nM) or later (H10-R 1 μM) during the process of *in vitro* selection of resistance.

environment of the T297M and P355S residue changes that are associated with azole resistance in *T. cruzi* clones, and hydrophobic contacts. Both positions appear in regions involved in the substrate binding and the catalytic action of the enzyme.

3.5. T297M replacement may reduce CYP51 affinity for anti-*T. cruzi* compounds

The drug binding sites presented in Fig. 6 effectively delineate the channel for drug and substrate access to the enzyme. Clearly, if an azole, imidazole or pyridine drug is chemotherapeutically active, the presence of drug bound in the channel or bound by its nitrogen to the 6th coordination site of the heme Fe⁺⁺, will reduce the ability of the enzyme to carry out its oxidative actions on the substrate. A random residue change in a channel leading to the active site, either to increase water-attraction with a new water attracting H-bond (such as P355S), or to reduce the space for water with increased hydrophobic bulk (such as T297M) may alter affinity for the drug and enable organisms with the mutated genome to proliferate.

It is unlikely that the T297M change directly interacts with the heme ring. The wild-type hydrophobic interactions of Thr295 help to stabilize the heme as shown in Fig. 6A. The Thr297 sidechain interacts with residues of an antiparallel more N-terminal alpha helix E. These links assist in positioning the Fe³⁺ of the heme drug target with respect to the basic N of the drug's azole group. Therefore, interaction of helices E and I can explain why the T297M residue change affects the activity of various azole drugs: both long side chained molecules, such

as posaconazole and itraconazole, and short side chained fluconazole.

Comparison of 3ksw.pdb deligated, before and after T297M residue change, showed weaker interactions between helices K and I (for example, L168 4.77 Å; C171 4.09 Å; G172 3.84 Å versus wild type (WT) L168 4.19 Å; C171 3.78 Å; G172 3.62 Å) (Fig. 6B–E).

4. Discussion

Here, we describe the generation of *T. cruzi* Y strain clones that developed stable resistance to ravuconazole *in vitro*, in intracellular amastigotes. Furthermore, we describe a novel CYP51 T297M amino acid change in the derived ravuconazole resistant *T. cruzi* clones. The models obtained predict the structural changes and their impact on interaction with azole and other CYP51 inhibitory drugs.

The T297M mutation identified is close to an enzyme active site that appears to have relevant effects on the efficiency of CYP51 inhibitory drugs. As the mutation is associated with a decrease in the therapeutic efficiency of azoles and fenarimols, the other class of anti-*T. cruzi* CYP51 drugs recently developed, we assume it restricts the access of the drug to the 6th coordination site of the iron in the spatially restricted area of the active site. Crucially, the structural change of residue 297 from Thr to Met in the drug resistant *T. cruzi* clones did not prevent the parasite growth *in vitro*, although it was associated with a remarkable decrease in fitness.

The decrease in fitness of the clone stock selected under the pressure of 500 nM ravuconazole was observed as slowed growth, decreased ratio of infected cells and (likely as a consequence of the former two) a reduced production of trypomastigotes from infected tissue cultures. The same phenotype of reduced growth was observed in epimastigotes, in addition to a deficient differentiation process from trypomastigotes into epimastigotes. Interestingly, this differentiation process did not occur in the presence of ravuconazole, even in the resistant clone, which suggests that either the mutated CYP51 is not expressed during the epimastigogenesis, or the resistant metabolism is not sufficient to overcome the higher recruitment of ergosterol during membrane remodelling – analogous to critical plasma membrane sterol organization observed in fungi (Sekiya and Nozawa, 1983; Prasad and Ghannoum, 1996) and plant embryogenesis (Schrack et al., 2000). The clones' fitness was also evaluated *in vivo*. It is noteworthy that all clones, regardless of the drug resistance background, presented much reduced virulence in comparison with the parental Y strain, suggesting that *in vitro* cultivation may have led to an attenuation of the highly virulent Y strain phenotype and/or the selected H10 clone was more adapted to *in vitro* culture. The only difference observed between sensitive and resistant clones *in vivo* was the delayed parasitemia peak observed in the resistant clones, suggesting that the mutation(s) that give rise to CYP51 inhibitors resistance caused slower/delayed replication in *T. cruzi in vivo*. Otherwise these clones remain viable and capable of establishing *in vivo* infection. Nevertheless, as the clones behave phenotypically similar *in vitro* and *in vivo*, it can be assumed that H10-R and H10-R-NP would also present ravuconazole resistance *in vivo*.

The T297M mutation has conferred resistance to ravuconazole, and other azoles and non-azole CYP51 inhibitors, but did not increase resistance to benznidazole, nifurtimox and the oxaborole AN4169. These data suggest that, should azoles become clinical drugs for the treatment of Chagas disease, single-point mutations could arise and eventually confer multidrug resistance to CYP51 inhibitors.

Interestingly, the clones selected for this study were more tolerant to benznidazole, when compared to most other *T. cruzi* strains (Franco et al., 2019; Moraes et al., 2014), in accordance with the tolerant phenotype reported for the Y strains by some, but not all studies (Filardi and Brener, 1987; Moraes et al., 2014; Campos et al., 2014; Palace-Berl et al., 2018), indicating that there might be considerable phenotypic (and genetic) variability among stocks of the Y strain from different laboratories. Another example of this variability is the fact that *T. cruzi* Y strain has been reported to possess two CYP51 genes: A and B, which

Table 5
Comparison of CYP51 protein amino acid residue positions throughout distinct *T. cruzi* strains.

<i>T. cruzi</i> strain	Amino acid residue														GenBank No	Notes	
	9	13	32	62	117	160	196	203	245	288	297	314	355	405			480
Tulahuen (TcVI)	A	L	P	D	A	E	H	K	V	A	T	K	P	D	P	AY283022	Allele 1
Tulahuen (TcVI)	A	L	P	E	S	K	H	K	V	A	T	K	P	D	P	AY283023	Allele 2
CL Brener (TcVI)	G	L	P	D	A	E	H	K	V	A	T	K	P	D	P	XM_815117	Genome sequence
CL Brener (TcVI)	A	L	P	E	S	K	H	K	V	A	T	K	P	D	P	XM_816126	Genome sequence
Tulahuen (TcVI)	G	L	P	D	A	E	H	K	V	A	T	K	P	D	P	AY856083	PCR primers reported here were based on this sequence
Silvio (Tcl)	C	L	P	D	S	K	R	K	I	A	T	K	P	E	P		Genome sequence
Colombiana (Tcl)	G	L	P	D	S	K	R	Q	I	A	T	E	P	E	S	KC330216	Gene A
Colombiana (Tcl)	A	P	S	E	S	K	H	K	V	S	T	K	P	D	P	KC330217	Gene B
Y (Tcll)	G	L	P	D	A	E	H	K	V	A	T	K	S ^a	D	P	JQ434483	Gene A; reported from resistant clone
Y (Tcll)	A	L	P	E	S	K	H	K	V	A	T	K	P	D	P	JQ434484	Gene B
Dm28c (Tcl)	C	L	P	D	S	K	R	K	I	A	T	K	P	E	P		Genome sequence
Y - H10 clone (Tcll)	A	L	P	E	S	K	H	K	V	A	T/M ^b	K	P	D	P		

^aYellow-highlighted cell indicates a previously reported mutation region. ^bGreen-highlighted cell marks the novel mutation region described here.

^aYellow-highlighted cell indicates a previously reported mutation region. ^bGreen-highlighted cell marks the novel mutation region described here.

are not 100% identical (Cherkesova et al., 2014). However, in this study, while we have identified two copies of CYP51 in the genome of the H10 clone. Both copies corresponded to the CYP51B gene previously reported, with the CYP51A gene not found. The differences in reported CYP51 copies between this study and the one published by Cherkesova and collaborators (Cherkesova et al., 2014) may be also attributed to variations in genetic composition of Y strains.

The natural tolerance to benzimidazole in *T. cruzi* is not yet well understood and has been attributed to upregulation of the ABCG1 transporter, while laboratory-selected benzimidazole resistance has been attributed to mutations in the *TcNTRI* gene (Wilkinson et al., 2008; Zingales et al., 2015; Campos et al., 2017). The natural tolerance to benzimidazole observed in the H10 clone did not seem to confer significant resistance/tolerance to CYP51 inhibitors, and the ravuconazole-resistant clones did not develop further tolerance or resistance to benzimidazole. As CYP51 inhibitors have been shown to display a variable spectrum of activity against different *T. cruzi* strains (Moraes et al., 2014), it would be of interest to investigate further whether the naturally resistant strains have variable CYP51 sequences that might help explaining their tolerance to azoles.

The resistant H10-R clone, in addition to show resistance to multiple antichagasic drugs and candidates (benzimidazole, azoles and fenarimols), presented slower growth and reduced infectivity, when compared to the parent sensitive H10-S clone. Due to these unique characteristics, the H10-S/H10-R Y strain clones might provide an interesting laboratory model for studies on drug mechanism of action and resistance in *T. cruzi*.

The reason why the T297M mutant present reduced fitness and whether it affects the function of the CYP51 enzyme is presently unknown. It is predictable that a change in one of the 34 signature

residues completely conserved throughout the eukaryotic CYP51 family (Hargrove et al., 2017) will not produce a viable drug-resistant parasite. Both the residue-changes, T297M and P355S, confirm this assumption. T297M immediately follows a consecutive series of 5 signature residues. P355 is 4 residues after the last signature residue R351 and appreciably before the next signature residue, R361. However, the position of the P355S residue change so close to the HT-pair functional in proton transfer may change the enzymatic activity.

The DUET protocol (Pires et al., 2014), was used on the CYP51 structure as advised by the website: <http://biosig.unimelb.edu.au/duet/stability>, after removing heme and drug ligands. The stabilising (+) or destabilising (−) ddG (delta delta Gibbs values in Kcal/mole) for residue changes were positive for T297M and negative for P355S. It was possible to examine 16 different strand A *T. cruzi* CYP51 crystal *.pdb structures from the RCSB database, with statistical analysis of the results. Residue change T297M was moderately stabilising (Mean ddg = 0.398563) SD = +- 0.138143, and P355S was overall quite destabilising (Mean ddg = -1.90744, SD = +- 0.188799). Particularly for enzymes, stabilising effects may affect function at least as much as destabilising. By analogy, a weakly stabilising change was observed for the enzyme dihydropteroate synthetase in *Plasmodium falciparum* resistant to sulfadoxine (Oguike et al., 2016). However, while T297M is apparently much less damaging than P355S, each of these residue changes is in a location where interference with the function of a Substrate Recognition Site can take place. The overall higher absolute value of the $\delta\delta G$ rating of P355S compared to the T297M variant, could also predict a fitness deficit for P355S, due to the more damaging nature of changing a highly conserved turn-defining residue in VdW contact with the heme.

Lepesheva and collaborators (Lepesheva et al., 2010), using a van

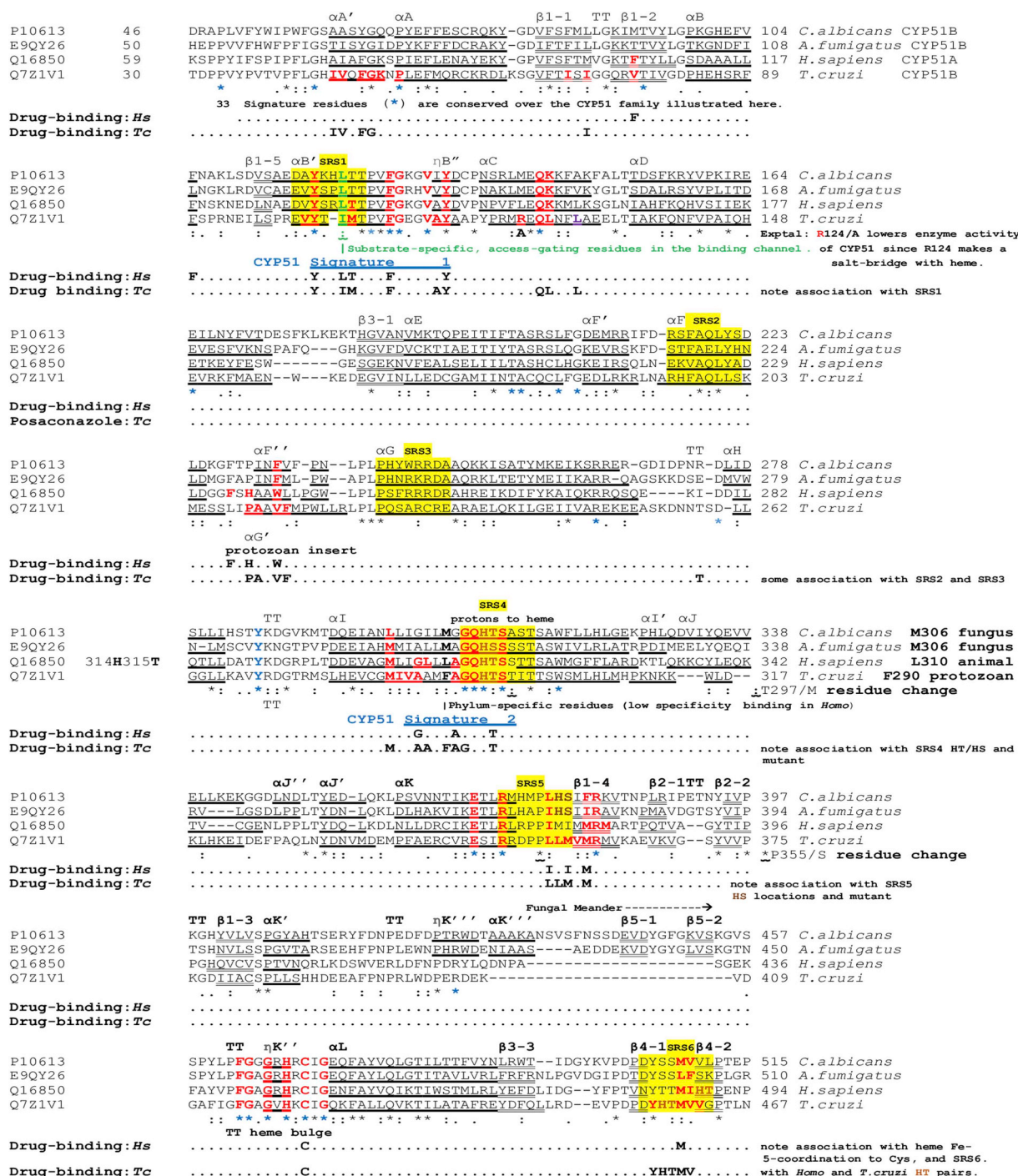


Fig. 5. Clustal O alignment of sterol 14 α -demethylase (CYP51) from parasitic Fungi, *Candida albicans* and *Aspergillus fumigatus*, in comparison with the *Homosapiens* and the parasitic *T. cruzi* enzymes. Residues in the CYP51 sterol-binding channel up to 4.5 Å from heme are bold red throughout. Drug-binding sites are noted in association with these residues. The α -helical and 310-helical η (*eta*)-sequences are bolded underlined, while β -strands are doubly underlined. TT indicates a turn, seen between parallel or antiparallel helices or β -strands, or in other locations, and usually indicates exposure of the turn residues to solvent. Six conserved Substrate Recognition Sites (Gotoh, 1992; Lepesheva and Waterman, 2011; Strushkevich et al., 2010) are located with a yellow background, arbitrarily including 8 residues and include SRS 4 with its His/Thr scouple in α -helix I, facilitating the delivery of protons (H⁺) to oxygenated heme in the substrate pocket. Histidine here is a conserved signature residue (*) which is followed by Thr or Ser, and immediately followed by the remainder of helix I. (For interpretation of the references to colour in this figure legend, the reader is referred to the Web version of this article.)

der Waals (VdW) distance of < 4.5 Å, noted that *T. cruzi* CYP51 α -helix I makes an important contribution to the deep hydrophobic active site cavity, specifically mentioning A287, F290, A291 and T295. We confirmed the hydrophobic interaction between: the first carbon of the sidechain (after C- α) of T295 (3.37 Å) and the heme; between Ala291 sidechain (2.85 Å) and the triazole ring of attached PSL [3k1o.pdb],

and between the side chain of Ala287/ring of F290 and the drug. We also observed, in comparison with *T. cruzi* and *T. brucei*, the non-helical more flexible region of the human α -helix I (A311, G312, Q313) in crystal structures 3jus.pdb and 3ld6.pdb, which potentially reduces the toxicity of azole compounds to humans. It is striking that, as demonstrated by Lepesheva and collaborators (Lepesheva et al., 2010), the

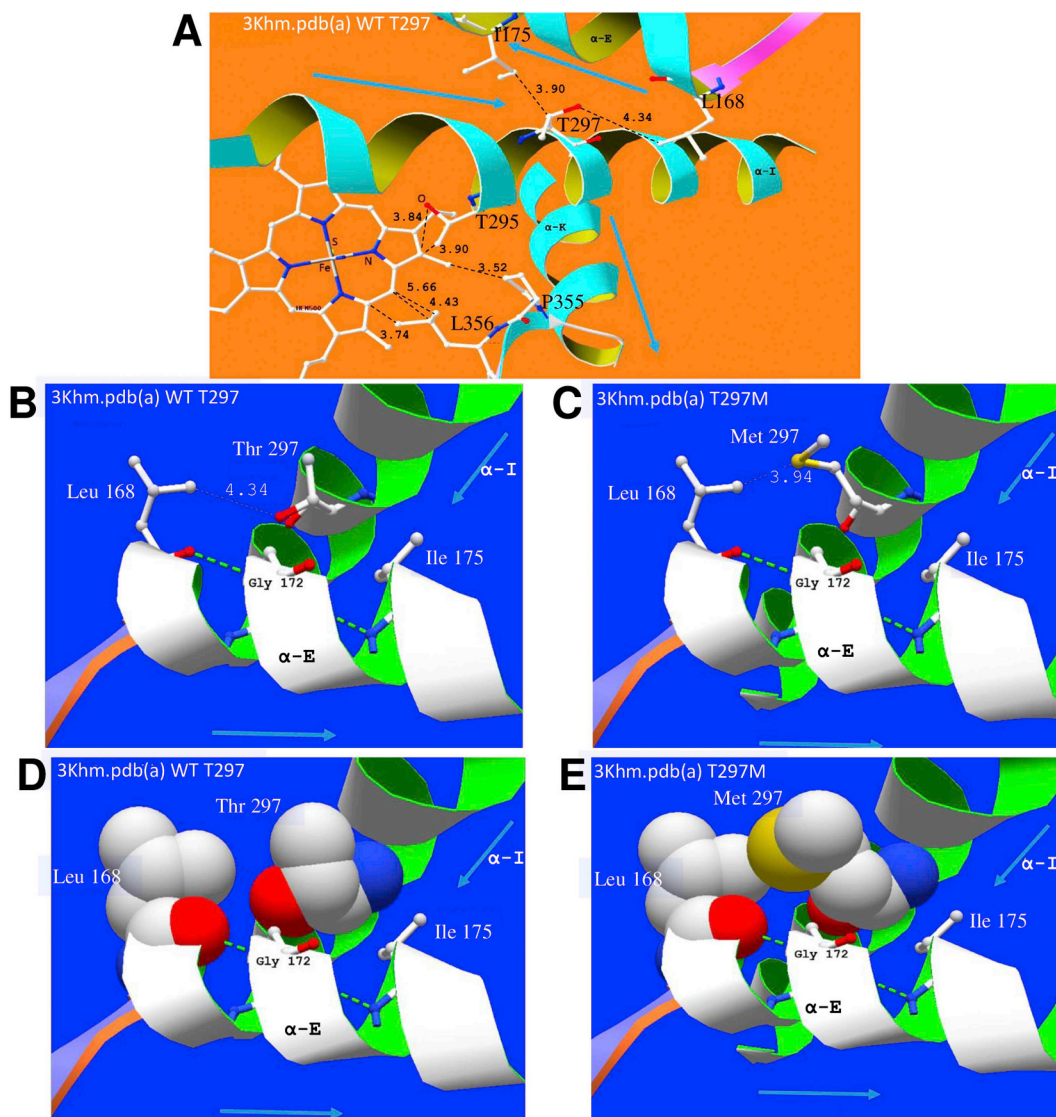


Fig. 6. Impact of residue changes T297M and P355S on the active site of CYP51. **A** (3khm.pdb (a) WT) The area around active site heme showing helix E and its VdW hydrophobic contact with signature helix I, through the side-chains of, for example, L168, I175 and T297/M297. This also shows helix K crossing helix I and supporting the following β -sheet bearing P355/S355 and L356, which support the heme. Helix I also supports heme through T295, among other residues. The residue change P355S replaces a highly conserved turn-defining residue in VdW hydrophobic contact with the heme and is next to residue L356, which also contacts heme. As can be seen from our alignment (Fig. 5) L356 binds all 7 drugs looked at in crystals of the *T. cruzi* - *T. brucei* enzyme. **B** and **C** show VdW distance change associated with T297M. **D** and **E** show the increased size of the sidechain of M297, four times more hydrophobic and 90 Å³ larger than that of T297, thus likely to reduce by 15% the solvent-accessible volume at the enzyme active site, estimated by Lepesheva and collaborators (Lepesheva et al., 2010) as 600 Å³ in *T. brucei*. This may hinder the access of drug to coordination at the 6th site of the heme iron as well as having some influence on access of the sterol substrate to the enzyme.

solvent accessible volume for each of the four enzyme molecules in the asymmetric unit of the *T. brucei* CYP51 enzyme approximates to only 600 Å³. In the absence of sterol substrate this 600 Å³ is occupied by water. The 600 Å³ is especially relevant to the impact on the active site, of replacement of T297 by M in α -helix I and the resultant different sidechain volume and hydrophobicity, particularly for the active site of *T. cruzi*. The residue numbers referred to here are identical for the CYP51 sequences of *T. brucei* and *T. cruzi*. It is notable from the comparative alignments (Fig. 5) that, after the entirely conserved Ser296 residue, position 297 is also highly conserved, as either Ser or Ala occurs across the eukaryotic CYP51 sequences, with residue hydrophobicities of 0.5, 3.3, respectively (and Thr, 3.9, for *Mycobacterium tuberculosis*, alignment not shown), Thr also being the residue in the *T. cruzi* H10-S/H10-LT clones. These three residues, as well as having low hydrophobicities ('stickiness') can also be seen to have relatively small sidechain volumes, of 241, 215 or 290 Å³, respectively. Of the three, only Ser and Thr may have sidechain H-bonding capability. However,

the hydrophobicity of the methionine residue that replaced the threonine 297 of the H10-R clones is 16, which is at least 4 times higher than Thr in the H10-S/H10-LT clones. Furthermore, the sidechain volume is 380 Å³, which is 90 Å³ higher. Thus, the *T. cruzi* residue 297 change from Thr to Met uses up 15% of the scarce 600 Å³ solvent accessible volume of the asymmetric CYP51 unit (Fig. 5 and Fig. S2).

It is notable that of seven drugs we have looked at in crystals of the *T. cruzi* or *T. brucei* enzyme (posaconazole, BS1246/UDO, BS967/UDO, fluconazole and imidazoles-VNF, VNI and VNV), all are bound by the L356, one to L357, 6/7 with M358 and 5/7 with M360. Cherkesova and collaborators (Cherkesova et al., 2014) reported that in CYP51A from Y strain of *T. cruzi*, where proline 355 was replaced by serine, rendered the parasite less sensitive to azole drug inhibition. They show by crystallography that in the usual CYP51B complex with drug VNI, proline 355 formed the surface of interaction with, for example, the carboxamide fragment of the drug, and they concluded that serine replacement for proline seen in CYP51A was likely to increase the

flexibility of that area of the drug-binding cavity. The enhanced likely inhibitory effect on enzyme function, also indicated by our DUET result, supports their conjecture. Change from Pro to Ser is likely to have an important effect on function of the enzyme. Some drug-resistant isolates of *Aspergillus (italicum, fischeri, fumigatus, clavatus and flavus)* also show this particular Pro to Ser residue change. There is an extensive literature regarding other mutations associated with azole-resistance in the fungal CYP51 (ERG11) gene. In *Aspergillus fumigatus*, a commonly reported mutation involves a tandem repeat (TR) of 34 or 46 bases within the promoter of the gene, reviewed by Chen and collaborators (Chen et al., 2020); parallel studies on *Candida albicans* have reported resistance-associated amino acid mutations that are principally localised within three different regions of the gene (reviewed by Warrilow et al., 2019; Zhang et al., 2019). Recent reports of mutations in CYP51/Erg11 associated with azole resistance in human pathogenic fungi are summarised in Table S3.

Because we cannot discard that other mutations might have occurred in other loci rendering the parasites more resistant, additional experiments such as genetic complementation of the wild-type *TcCYP51* in the resistant clones, substitution of the wild-type endogenous copy with the T297M *TcCYP51* and/or assessment of enzymatic activity of 297M *TcCYP51*, would also help elucidating the role of this mutation in the resistance to CYP51 inhibitors. Additional progressive mutation, other genetic mechanisms or non-genetic metabolic mechanisms may be involved, such as those implicated in the development of drug resistance in the malaria parasite, *Plasmodium falciparum* (Herman et al., 2014). Also, the fact that H10-R-NP clone has partially recovered *in vitro* fitness and presents a lower EC₅₀ values for azole drugs (in comparison to H10-R clone), corroborates for the occurrence of transient/adaptative mutations and/or non-genetic alterations which were not detected within the target site. To investigate the presence of other mechanisms, we are in the process of comparing the Illumina genome sequences of all the resistant clones against a high resolution PacBio genome scaffold of the source susceptible Y strain.

5. Conclusion

A ravuconazole resistant clone of *T. cruzi* (Y strain) was selected *in vitro*. In comparison with the parental clone, the resistant clone presented reduced fitness, low infectivity and a slow epimastigote differentiation process. The clone was cross-resistant to several CYP51 inhibitors (azoles and fenarimols), but not to benzimidazole, nifurtimox, oxaborole or amphotericin B. The phenotypic changes observed in the resistant clones were not due to prolonged *in vitro* culture and could not be reversed by removing drug pressure or after a completing an *in vitro* life cycle. A novel residue change T297M was identified in the CYP51 of the resistant clones. Comparative amino acid sequence alignments and modelling of crystal structures suggested that T297M has a structural impact that affect the enzyme capacity of binding to azole inhibitors, as the previously described P355S mutation.

Declaration of competing interest

The authors declare that they have no conflicts of interest with the contents of this article. The donors had no role in study design, data collection and analysis, decision to publish, or preparation of the manuscript.

Acknowledgments

The authors would like to thank Luisa Naves, Hwayoung Kim and Luis Gaspar for technical support with *in vitro* cultures. The authors would like also to thank Eisai, Ltd., for providing ravuconazole, Epichem Pty, Ltd. for providing nifurtimox, AN4169/EPL-BS497, posaconazole, EPL-BS967 and EPL-BS1246. This study was funded by

DNDi and the Institut Pasteur Korea (IPK). For the work described in this paper, DNDi received financial support from the Reconstruction Credit Institution-Federal Ministry of Education and Research (KfW-BMBF)/Germany; Médecins Sans Frontières (Doctors without Borders)/International; Department for International Development (DFID), UK; Directorate-General for International Cooperation (DGIS), The Netherlands; and Swiss Agency for Development and Cooperation (SDC). IPK received a National Research Foundation of Korea (NRF) grant funded by the Korean government (MSIP No. 2007-00559), Gyeonggi-do and KISTI.

Appendix A. Supplementary data

Supplementary data to this article can be found online at <https://doi.org/10.1016/j.ijpddr.2020.06.001>.

References

- Antinori, S., Galimberti, L., Bianco, R., Grande, R., Galli, M., Corbellino, M., 2017. Chagas disease in Europe: a review for the internist in the globalized world. *Eur. J. Intern. Med.* 43, 6–15. <https://doi.org/10.1016/j.ejim.2017.05.001>.
- Borst, P., Ouellette, M., 1995. New mechanisms of drug resistance in parasitic protozoa. *Annu. Rev. Microbiol.* 49, 427–460. <https://doi.org/10.1146/annurev.mi.49.100195.002235>.
- Buckner, F.S., Joubert, B.M., Boyle, S.M., Eastman, R.T., Verlinde, C.L.M.J., Matsuda, S.P.T., 2003. Cloning and analysis of *Trypanosoma cruzi* lanosterol 14 α -demethylase. *Mol. Biochem. Parasitol.* 132, 75–81. <https://doi.org/10.1016/j.molbiopara.2003.07.004>.
- Buckner, F.S., Wilson, A.J., White, T.C., Van Voorhis, W.C., 1998. Induction of resistance to azole drugs in *Trypanosoma cruzi*. *Antimicrob. Agents Chemother.* 42, 3245–3250.
- Camargo, E.P., 1964. Growth and differentiation in *Trypanosoma cruzi*. I. Origin of metacyclic trypanosomes in liquid media. *Rev. Inst. Med. Trop. Sao Paulo* 93–100.
- Campos, M.C., Phelan, J., Francisco, A.F., Taylor, M.C., Lewis, M.D., Pain, A., Clark, T.G., Kelly, J.M., 2017. Genome-wide mutagenesis and multi-drug resistance in American trypanosomes induced by the front-line drug benzimidazole. *Sci. Rep.* 7, 14407. <https://doi.org/10.1038/s41598-017-14986-6>.
- Campos, M.C.O., Leon, L.L., Taylor, M.C., Kelly, J.M., 2014. Benzimidazole-resistance in *Trypanosoma cruzi*: evidence that distinct mechanisms can act in concert. *Mol. Biochem. Parasitol.* 193, 17–19. <https://doi.org/10.1016/j.molbiopara.2014.01.002Shortcommunication>.
- Cencig, S., Coltel, N., Truysens, C., Carlier, Y., 2011. Parasitic loads in tissues of mice infected with *Trypanosoma cruzi* and treated with AmBisome. *PLoS Neglected Trop. Dis.* 5, e1216. <https://doi.org/10.1371/journal.pntd.0001216>.
- Chen, P., Liu, M., Zeng, Q., Zhang, Z., Liu, W., Sang, H., Lu, L., 2020. Uncovering new mutations conferring azole resistance in the *Aspergillus fumigatus* cyp51A gene. *Front. Microbiol.* 10, 3127. <https://doi.org/10.3389/fmicb.2019.03127>.
- Cherkesova, T.S., Hargrove, T.Y., Vanrell, M.C., Ges, I., Usanov, S.A., Romano, P.S., Lepesheva, G.I., 2014. Sequence variation in CYP51A from the Y strain of *Trypanosoma cruzi* alters its sensitivity to inhibition. *FEBS Lett.* 588, 3878–3885. <https://doi.org/10.1016/j.febslet.2014.08.030>.
- Clemons, K.V., Sobel, R.A., Martinez, M., Correa-Oliveira, R., Stevens, D.A., 2017. Lack of efficacy of liposomal amphotericin B against acute and chronic *Trypanosoma cruzi* infection in mice. *Am. J. Trop. Med. Hyg.* 97, 1141–1146. <https://doi.org/10.4269/ajtmh.16-0975>.
- Daniels, J.-P., Gull, K., Wickstead, B., 2010. Cell biology of the trypanosome genome. *Microbiol. Mol. Biol. Rev.* 74, 552–569. <https://doi.org/10.1128/MMBR.00024-10>.
- De-Castro, S., Soeiro, M., Higashi, K., Meirelles, M., 1993. Differential effect of amphotericin B on the three evolutive stages of *Trypanosoma cruzi* and on the host cell-parasite interaction. *Braz. J. Med. Biol. Res.* 26, 1219–1229.
- Di Noia, J.M., Buscaglia, C. a, De Marchi, C.R., Almeida, I.C., Frasch, A.C.C., 2002. A *Trypanosoma cruzi* small surface molecule provides the first immunological evidence that Chagas' disease is due to a single parasite lineage. *J. Exp. Med.* 195, 401–413. <https://doi.org/10.1084/jem.20011433>.
- El-Sayed, N.M., Myler, P.J., Bartholomeu, D.C., Nilsson, D., Aggarwal, G., Tran, A.-N., Ghedin, E., Worthey, E.A., Delcher, A.L., Blandin, G., Westenberg, S.J., Caler, E., Cerqueira, G.C., Branche, C., Haas, B., Anupama, A., Arner, E., Aslund, L., Attipoe, P., Bontempi, E., Bringaud, F., Burton, P., Cadag, E., Campbell, D.A., Carrington, M., Crabtree, J., Darban, H., da Silveira, J.F., de Jong, P., Edwards, K., Englund, P.T., Fazelina, G., Feldblyum, T., Ferella, M., Frasch, A.C., Gull, K., Horn, D., Hou, L., Huang, Y., Kindlund, E., Klingbeil, M., Kluge, S., Koo, H., Lacerda, D., Levin, M.J., Lorenzi, H., Louie, T., Machado, C.R., McCulloch, R., McKenna, A., Mizuno, Y., Mottram, J.C., Nelson, S., Ochaya, S., Soegawa, K., Pai, G., Parsons, M., Pentony, M., Pettersson, U., Pop, M., Ramirez, J.L., Rinta, J., Robertson, L., Salzberg, S.L., Sanchez, D.O., Seyler, A., Sharma, R., Shetty, J., Simpson, A.J., Sisk, E., Tammi, M.T., Tarleton, R., Teixeira, S., Van Aken, S., Vogt, C., Ward, P.N., Wickstead, B., Wortman, J., White, O., Fraser, C.M., Stuart, K.D., Andersson, B., 2005. The genome sequence of *Trypanosoma cruzi*, etiologic agent of Chagas disease. *Science* 309, 409–415. <https://doi.org/10.1126/science.1112631>.
- Filardi, L.S., Brener, Z., 1987. Susceptibility and natural resistance of *Trypanosoma cruzi* strains to drugs used clinically in Chagas disease. *Trans. R. Soc. Trop. Med. Hyg.* 81,

- 755–759. [https://doi.org/10.1016/0035-9203\(87\)90020-4](https://doi.org/10.1016/0035-9203(87)90020-4).
- Francisco, A.F., Lewis, M.D., Jayawardhana, S., Taylor, M.C., Chatelain, E., Kelly, J.M., 2015. Limited ability of posaconazole to cure both acute and chronic *Trypanosoma cruzi* infections revealed by highly sensitive in vivo imaging. *Antimicrob. Agents Chemother.* 59, 4653–4661. <https://doi.org/10.1128/AAC.00520-15>.
- Franco, C.H., Alcântara, L.M., Chatelain, E., Freitas-Junior, L., Moraes, C.B., 2019. Drug discovery for Chagas disease: impact of different host cell lines on assay performance and hit compound selection. *Trav. Med. Infect. Dis.* 4, 82. <https://doi.org/10.3390/tropicalmed4020082>.
- Franzén, O., Ochaya, S., Sherwood, E., Lewis, M.D., Llewellyn, M.S., Miles, M.A., Andersson, B., 2011. Shotgun sequencing analysis of *Trypanosoma cruzi* I Sylvio X10/1 and comparison with *T. cruzi* VI CL Brener. *PLoS Neglected Trop. Dis.* 5, e984. <https://doi.org/10.1371/journal.pntd.0000984>.
- Goad, L.J., Berens, R.L., Marr, J.J., Beach, D.H., Holz, G.G., 1989. The activity of ketoconazole and other azoles against *Trypanosoma cruzi*: biochemistry and chemotherapeutic action in vitro. *Mol. Biochem. Parasitol.* 32, 179–189.
- Gotoh, O., 1992. Substrate recognition sites in cytochrome P450 family 2 (CYP2) proteins inferred from comparative analyses of amino acid and coding nucleotide sequences. *J. Biol. Chem.* 267, 83–90.
- Grisard, E.C., Teixeira, S.M.R., de Almeida, L.G.P., Stoco, P.H., Gerber, A.L., Talavera-López, C., Lima, O.C., Andersson, B., de Vasconcelos, A.T.R., 2014. *Trypanosoma cruzi* clone Dm28c draft genome sequence. *Genome Announc.* 2. <https://doi.org/10.1128/genomeA.01114-13>. e01114-13.e01114-13.
- Gulin, J.E.N., Eagleson, M. a, Postan, M., Cutrullis, R. a, Freilij, H., Bourmisen, F.G., Petray, P.B., Altcheh, J., 2013. Efficacy of voriconazole in a murine model of acute *Trypanosoma cruzi* infection. *J. Antimicrob. Chemother.* 68, 888–894. <https://doi.org/10.1093/jac/dks478>.
- Haido, R.M., Barreto-Bergter, E., 1989. Amphotericin B-induced damage of *Trypanosoma cruzi* epimastigotes. *Chem. Biol. Interact.* 71, 91–103.
- Hall, T.A., 1999. BioEdit: a user friendly biological sequence alignment editor and analysis program for Windows 95/98/NT. *Nucleic Acids Symp. Ser.* 41, 95–98.
- Hargrove, T.Y., Friggeri, L., Wawrzak, Z., Qi, A., Hoekstra, W.J., Schotzinger, R.J., York, J.D., Peter Guengerich, F., Lepesheva, G.I., 2017. Structural analyses of *Candida albicans* sterol 14 α -demethylase complexed with azole drugs address the molecular basis of azole-mediated inhibition of fungal sterol biosynthesis. *J. Biol. Chem.* 292, 6728–6743. <https://doi.org/10.1074/jbc.M117.778308>.
- Hargrove, T.Y., Wawrzak, Z., Alexander, P.W., Chaplin, J.H., Keenan, M., Charman, S.A., Perez, C.J., Waterman, M.R., Chatelain, E., Lepesheva, G.I., 2013. Complexes of *Trypanosoma cruzi* sterol 14 α -demethylase (CYP51) with two pyridine-based drug candidates for Chagas disease: structural basis for pathogen selectivity. *J. Biol. Chem.* 288, 31602–31615. <https://doi.org/10.1074/jbc.M113.497990>.
- Herman, J.D., Rice, D.P., Ribacke, U., Silterra, J., Deik, A.A., Moss, E.L., Broadbent, K.M., Neafsey, D.E., Desai, M.M., Clish, C.B., Mazitschek, R., Wirth, D.F., 2014. A genomic and evolutionary approach reveals non-genetic drug resistance in malaria. *Genome Biol.* 15, 511. <https://doi.org/10.1186/s13059-014-0511-2>.
- Keenan, M., Abbott, M.J., Alexander, P.W., Armstrong, T., Best, W.M., Berlan, B., Botero, A., Chaplin, J.H., Charman, S.A., Chatelain, E., von Geldern, T.W., Kerfoot, M., Khong, A., Nguyen, T., McManus, J.D., Morizzi, J., Ryan, E., Scandale, I., Thompson, R.A., Wang, S.Z., White, K.L., 2012. Analogues of fenarimol are potent inhibitors of *Trypanosoma cruzi* and are efficacious in a murine model of Chagas disease. *J. Med. Chem.* 55, 4189–4204. <https://doi.org/10.1021/jm20155809>.
- Khare, S., Liu, X., Stinson, M., Rivera, I., Groessl, T., Tuntland, T., Yeh, V., Wen, B., Molteni, V., Glynn, R., Supek, F., 2015. Antitrypanosomal treatment with benznidazole is superior to posaconazole regimens in mouse models of Chagas disease. *Antimicrob. Agents Chemother.* 59, 6385–6394. <https://doi.org/10.1128/AAC.00689-15>.
- Kovacs, J.M., Mant, C.T., Hodges, R.S., 2006. Determination of intrinsic hydrophilicity/hydrophobicity of amino acid side chains in peptides in the absence of nearest-neighbor or conformational effects. *Biomolecules* 84, 283–297. <https://doi.org/10.1002/bip.20417>.
- Lee, B.Y., Bacon, K.M., Bottazzi, M.E., Hotez, P.J., 2013. Global economic burden of Chagas disease: a computational simulation model. *Lancet Infect. Dis.* 13, 342–348. [https://doi.org/10.1016/S1473-3099\(13\)70002-1](https://doi.org/10.1016/S1473-3099(13)70002-1).
- Lepesheva, G., Park, H.-W., Hargrove, T., Vanhollenbeke, B., Wawrzak, Z., Harp, J., Sundaramoorthy, M., Nes, W.D., Pays, E., Chaudhuri, M., Villalta, F., Waterman, M., 2010. Crystal structures of *Trypanosoma brucei* sterol 14 α -demethylase and implications for selective treatment of human infections. *J. Biol. Chem.* 285, 1773–1780. <https://doi.org/10.1074/jbc.M109.067470>.
- Lepesheva, G.I., Waterman, M.R., 2011. Sterol 14 α -demethylase (CYP51) as a therapeutic target for human trypanosomiasis and leishmaniasis. *Curr. Top. Med. Chem.* 11, 2060–2071. <https://doi.org/10.2174/156802611796575902>.
- Lepesheva, G.I., Waterman, M.R., 2007. Sterol 14 α -demethylase cytochrome P450 (CYP51), a P450 in all biological kingdoms. *Biochim. Biophys. Acta Gen. Subj.* 1770, 467–477. <https://doi.org/10.1016/j.bbagen.2006.07.018>.
- Lepesheva, G.I., Zaitseva, N.G., Nes, W.D., Zhou, W., Arase, M., Liu, J., Hill, G.C., Waterman, M.R., 2006. CYP51 from *Trypanosoma cruzi*: a phylo-specific residue in the B' helix defines substrate preferences of sterol 14 α -demethylase. *J. Biol. Chem.* 281, 3577–3585. <https://doi.org/10.1074/jbc.M510317200>.
- Lewis, M.D., Ma, J., Yeo, M., Carrasco, H.J., Llewellyn, M.S., Miles, M.A., Lewis, M.D., Yeo, M., Ma, J., Miles, M.A., Llewellyn, M.S., 2009. Genotyping of *Trypanosoma cruzi*: systematic selection of assays allowing rapid and accurate discrimination of all known lineages. *Am. J. Trop. Med. Hyg.* 81, 1041–1049. <https://doi.org/10.4269/ajtmh.2009.09-0305>.
- McCabe, R.E., Remington, J.S., Araujo, F.G., 1986. In vitro and in vivo effects of itraconazole against *Trypanosoma cruzi*. *Am. J. Trop. Med. Hyg.* 35, 280–284.
- Molina, I., Gómez i Prat, J., Salvador, F., Treviño, B., Sulleiro, E., Serre, N., Pou, D., Roure, S., Cabezas, J., Valerio, L., Blanco-Grau, A., Sánchez-Montalvá, A., Vidal, X., Pahissa, A., 2014. Randomized trial of posaconazole and benznidazole for chronic Chagas' disease. *N. Engl. J. Med.* 370, 1899–1908. <https://doi.org/10.1056/NEJMoa1313122>.
- Moraes, C.B., Franco, C.H., 2016. Novel drug discovery for Chagas disease. *Exp. Opin. Drug Discov.* 11, 447–455. <https://doi.org/10.1517/17460441.2016.1160883>.
- Moraes, C.B., Giardini, M.A., Kim, H., Franco, C.H., Araujo-Junior, A.M., Schenkman, S., Chatelain, E., Freitas-Junior, L.H., 2014. Nitroheterocyclic compounds are more efficacious than CYP51 inhibitors against *Trypanosoma cruzi*: implications for Chagas disease drug discovery and development. *Sci. Rep.* 4, 4703. <https://doi.org/10.1038/srep04703>.
- Morillo, C.A., Marin-Neto, J.A., Avezum, A., Sosa-Estani, S., Rassi, A., Rosas, F., Villena, E., Quiroz, R., Bonilla, R., Britto, C., Guhl, F., Velazquez, E., Bonilla, L., Meeks, B., Rao-Melacini, P., Pogue, J., Mattos, A., Lazzini, J., Rassi, A., Connolly, S.J., Yusuf, S., BENEFIT Investigators, 2015. Randomized trial of benznidazole for chronic Chagas' cardiomyopathy. *N. Engl. J. Med.* 373, 1295–1306. <https://doi.org/10.1056/NEJMoa1507574>.
- Morillo, C.A., Waskin, H., Sosa-Estani, S., del Carmen Bangher, M., Cuneo, C., Milesi, R., Mallagry, M., Apt, Werner, Beloscar, J., Gascon, Joaquim, Molina, Israel, Echeverría, L.E., Colombo, Hugo, Perez-Molina, Jose, Antonio, Wyss, F., Meeks, B., Bonilla, L.R., Gao, P., Wei, B., McCarthy, M., Yusuf, S., Morillo, C., Sosa-Estani, S., Waskin, H., Meeks, B., Yusuf, S., Diaz, R., Acquatella, H., Lazzari, J., Roberts, R., Traina, M., Meeks, B., Bonilla, L.R., Gao, P., Taylor, A., Holadyk-Gris, I., Whalen, L., Bangher, M.C., Romero, M.A., Prado, N., Hernández, Y., Fernandez, M., Riarte, A., Scollo, K., Lopez-Albizu, C., Cuneo, C.A., Gutiérrez, N.C., Milesi, R.R., Berli, M.A., Mallagry, M.H., Cáceres, N.E., Beloscar, J.S., Petrucci, J.M., Colombo, H., Dellatorre, M., Prado, A., Apt, W., Zulantay, I., Echeverría, L.E., Isaza, D., Reyes, E., Wyss, F.S., Figueroa, A., Guzmán Melgar, I., Rodríguez, E., Gascon, J., Aldasoro, E., Posada, E.J., Serret, N., Molina, I., Sánchez-Montalvá, A., Perez-Molina, J.A., López-Vélez, R., Reyes-López, P.A., 2017. Benznidazole and posaconazole in eliminating parasites in asymptomatic *T. cruzi* carriers: the STOP-CHAGAS trial. *J. Am. Coll. Cardiol.* 69, 939–947. <https://doi.org/10.1016/j.jacc.2016.12.023>.
- Oguike, M.C., Falade, C.O., Shu, E., Enato, I.G., Watila, I., Baba, E.S., Bruce, J., Webster, J., Hamade, P., Meek, S., Chandramohan, D., Sutherland, C.J., Warhurst, D., Roper, C., 2016. Molecular determinants of sulfadoxine-pyrimethamine resistance in *Plasmodium falciparum* in Nigeria and the regional emergence of dhps 431V. *Int. J. Parasitol. Drugs Drug Resist.* 6, 220–229. <https://doi.org/10.1016/j.ijpddr.2016.08.004>.
- Palace-Berl, F., Pasqualoto, K.F.M., Zingales, B., Moraes, C.B., Bury, M., Franco, C.H., da Silva Neto, A.L., Murayama, J.S., Nunes, S.L., Silva, M.N., Tavares, L.C., 2018. Investigating the structure-activity relationships of N'-(5-nitrofuranyl-2-yl) methylene substituted hydrazides against *Trypanosoma cruzi* to design novel active compounds. *Eur. J. Med. Chem.* 144, 29–40. <https://doi.org/10.1016/j.ejmech.2017.12.011>.
- Pérez-Molina, J. a, Pérez-Ayala, A., Moreno, S., Fernández-González, M.C., Zamora, J., López-Vélez, R., 2009. Use of benznidazole to treat chronic Chagas' disease: a systematic review with a meta-analysis. *J. Antimicrob. Chemother.* 64, 1139–1147. <https://doi.org/10.1093/jac/dkp357>.
- Pérez-Molina, J.A., Molina, I., 2018. Chagas disease. *Lancet* 391, 82–94. [https://doi.org/10.1016/S0140-6736\(17\)31612-4](https://doi.org/10.1016/S0140-6736(17)31612-4).
- Pires, D.E.V., Ascher, D.B., Blundell, T.L., 2014. DUET: a server for predicting effects of mutations on protein stability using an integrated computational approach. *Nucleic Acids Res.* 42, W314–W319. <https://doi.org/10.1093/nar/gku411>.
- Prasad, R., Ghannoum, M.A., 1996. *Lipids of Pathogenic Fungii*. CRC Press, Boca Raton.
- Purkait, B., Kumar, A., Nandi, N., Sardar, A.H., Das, S., Kumar, S., Pandey, K., Ravidas, V., Kumar, M., De, T., Singh, D., Das, P., 2012. Mechanism of amphotericin B resistance in clinical isolates of *Leishmania donovani*. *Antimicrob. Agents Chemother.* 56, 1031–1041. <https://doi.org/10.1128/AAC.00030-11>.
- Schrick, K., Mayer, U., Horrichs, A., Kuhn, C., Bellini, C., Dangel, J., Schmidt, J., Jürgens, G., 2000. FACKEL is a sterol C-14 reductase required for organized cell division and expansion in Arabidopsis embryogenesis. *Genes Dev.* 14, 1471–1484. <https://doi.org/10.1101/gad.14.12.1471>.
- Sekiya, T., Nozawa, Y., 1983. Reorganization of membrane ergosterol during cell fission events of *Candida albicans*: a freeze-fracture study of distribution of filipin-ergosterol complexes. *J. Ultrastruct. Res.* 83, 48–57. [https://doi.org/10.1016/S0022-5320\(83\)90064-3](https://doi.org/10.1016/S0022-5320(83)90064-3).
- Silva, F.T., Franco, C.H., Favaro, D.C., Freitas-Junior, L.H., Moraes, C.B., Ferreira, E.I., 2016. Design, synthesis and antitrypanosomal activity of some nitrofurazone 1,2,4-triazolico bioisosteric analogues. *Eur. J. Med. Chem.* 121, 553–560. <https://doi.org/10.1016/j.ejmech.2016.04.065>.
- Soeiro, M. de N., de Souza, E.M., da Silva, C.F., Batista, D. da G.J., Batista, M.M., Pavão, B.P., Araújo, J.S., Aiub, C.A.F., da Silva, P.B., Lionel, J., Britto, C., Kim, K., Sulikowski, G., Hargrove, T.Y., Waterman, M.R., Lepesheva, G.I., 2013. In vitro and in vivo studies of the antiparasitic activity of sterol 14 α -demethylase (CYP51) inhibitor VNI against drug-resistant strains of *Trypanosoma cruzi*. *Antimicrob. Agents Chemother.* 57, 4151–4163. <https://doi.org/10.1128/AAC.00070-13>.
- Strushkevich, N., Usanov, S.A., Park, H.-W., 2010. Structural basis of human CYP51 inhibition by antifungal azoles. *J. Mol. Biol.* 397, 1067–1078. <https://doi.org/10.1016/j.jmb.2010.01.075>.
- Urbina, J.A., 2010. Specific chemotherapy of Chagas disease: relevance, current limitations and new approaches. *Acta Trop.* 115, 55–68. <https://doi.org/10.1016/j.actatropica.2009.10.023>.
- Urbina, J.A., Payares, G., Sanoja, C., Lira, R., Romanha, A.J., 2003. In vitro and in vivo activities of ravuconazole on *Trypanosoma cruzi*, the causative agent of Chagas disease. *Int. J. Antimicrob. Agents* 21, 27–38. [https://doi.org/10.1016/S0924-8579\(02\)00273-X](https://doi.org/10.1016/S0924-8579(02)00273-X).

- Velazquez, E., Meeks, B., Bonilla, L., Rassi, A., Bonilla, R., Lazdins, J., Pogue, J., Sosa-Estani, S., Rao-Melacini, P., Britto, C., Rosas, F., Avezum, A., Mattos, A., Marin-Neto, J.A., Connolly, S.J., Villena, E., Quiroz, R., Morillo, C.A., Yusuf, S., Guhl, F., Marin-Neto, J.A., Avezum, A., Sosa-Estani, S., Rassi, A., Rosas, F., Villena, E., Quiroz, R., Bonilla, R., Britto, C., Guhl, F., Velazquez, E., Bonilla, L., Meeks, B., Rao-Melacini, P., Pogue, J., Mattos, A., Lazdins, J., Rassi, A., Connolly, S.J., Yusuf, S., 2015. Randomized trial of benznidazole for chronic Chagas' cardiomyopathy. *N. Engl. J. Med.* 373, 1295–1306. <https://doi.org/10.1056/NEJMoa1507574>.
- Viotti, R., Vigliano, C., Lococo, B., Bertocchi, G., Petti, M., Alvarez, M.G., Postan, M., Armenti, A., 2006. Long-term cardiac outcomes of treating chronic Chagas disease with benznidazole versus no treatment: a nonrandomized trial. *Ann. Intern. Med.* 144, 724–734. <https://doi.org/10.7326/0003-4819-144-10-200605160-00006>.
- Warrilow, A.G., Nishimoto, A.T., Parker, J.E., Price, C.L., Flowers, S.A., Kelly, D.E., Rogers, P.D., Kelly, S.L., 2019. The evolution of azole resistance in *Candida albicans* sterol 14 α -demethylase (CYP51) through incremental amino acid substitutions. *Antimicrob. Agents Chemother.* 63. <https://doi.org/10.1128/AAC.02586-18>.
- WHO, 2013. *Sustaining the Drive to Overcome the Global Impact of Neglected Tropical Diseases, Second WHO Report on Neglected Tropical Diseases*. WHO Press, Geneva.
- Wilkinson, S.R., Taylor, M.C., Horn, D., Kelly, J.M., Cheeseman, I., 2008. A mechanism for cross-resistance to nifurtimox and benznidazole in trypanosomes. *Proc. Natl. Acad. Sci. U.S.A.* 105, 5022–5027. <https://doi.org/10.1073/pnas.0711014105>.
- Yardley, V., Croft, S.L., 1999. In vitro and in vivo activity of amphotericin B-lipid formulations against experimental *Trypanosoma cruzi* infections. *Am. J. Trop. Med. Hyg.* 61, 193–197. <https://doi.org/10.4269/ajtmh.1999.61.193>.
- Yuan, G., 2012. DNA Submission Guidance for PacBio SMRT Sequencing. [WWW Document]. URL <https://www.pacb.com/wp-content/uploads/Technical-Note-Preparing-Samples-for-PacBio-Whole-Genome-Sequencing-for-de-novo-Assembly-Collection-and-Storage.pdf> accessed 4.20.17.
- Yun, O., Lima, M.A., Ellman, T., Chambi, W., Castillo, S., Flevaud, L., Roddy, P., Parreño, F., Albajar Viñas, P., Palma, P.P., 2009. Feasibility, drug safety, and effectiveness of etiological treatment programs for Chagas disease in Honduras, Guatemala, and Bolivia: 10-year experience of Médecins Sans Frontières. *PLoS Neglected Trop. Dis.* 3, e488. <https://doi.org/10.1371/journal.pntd.0000488>.
- Zhang, J., Li, L., Lv, Q., Yan, L., Wang, Y., Jiang, Y., 2019. The fungal CYP51s: their functions, structures, related drug resistance, and inhibitors. *Front. Microbiol.* 10, 691. <https://doi.org/10.3389/fmicb.2019.00691>.
- Zingales, B., Araujo, R.G.A., Moreno, M., Franco, J., Aguiar, P.H.N., Nunes, S.L., Silva, M.N., Ienne, S., Machado, C.R., Brandão, A., 2015. A novel ABCG-like transporter of *Trypanosoma cruzi* is involved in natural resistance to benznidazole. *Mem. Inst. Oswaldo Cruz* 110, 433–444. <https://doi.org/10.1590/0074-02760140407>.